to be G0 cells [24]. Pyronin Y and Hoechst double staining shows that approximately 90% of fresh SM/C-2.6$^+$ cells were in the G0 phase of the cell cycle. In contrast, 90% of cultured SM/C-2.6$^+$ cells were cycling (Fig. 1E).

Thus, our procedure, which takes 5–6 hours in total to isolate 1–2 × $10^5$ SM/C-2.6$^+$ cells from one C57BL/6 mouse, enables us to isolate satellite cells still in a quiescent and undifferentiated state. The yield corresponds to 10%–15% of the total mononucleated cells obtained from mouse hind limb muscles by enzymatic digestion. Therefore, in this report, we call freshly isolated SM/C-2.6$^+$ cells "quiescent satellite cells" and cultured, proliferating SM/C-2.6$^+$ cells "activated satellite cells." Our procedure was also applicable to dystrophin-deficient *mdx* muscle with modifications, although 30%–40% of *mdx* satellite cells are Ki67-positive (M. Ikemoto et al., submitted manuscript). Unfortunately, SM/C-2.6 did not react with satellite cells from dystrophin-deficient dystrophic dogs (data not shown).

## Single Gene Analysis of Quiescent and Activated/Proliferating Satellite Cells

We prepared RNA samples from quiescent satellite cells and activated satellite cells and performed microarray analysis using Affymetrix GeneChips. Hybridization and data collection were performed four times using independent preparations of cells and RNA samples for each cell fraction. Raw data are available at http://www.ncbi.nlm.nih.gov/geo. The Gene Expression Omnibus accession number is GSE3483.

First, we compared the expression levels of individual genes in quiescent and activated states using GeneSpring software. We found that 507 genes (665 probes) were expressed in quiescent satellite cells at more than fivefold higher levels than in activated satellite cells (Fig. 2A). We roughly categorized these 507 genes into 11 gene groups: cell adhesion (15 genes), cell cycle regulation (26), proteolysis (21), cytoskeleton (13), cell surface (41), extracellular (61), immunoresponse (22), signal transduction (81), transcription (67), transport and metabolism (82), and unknown (78) based on Gene Ontology and listed all of them in supplemental online Table 1. On the other hand, 659 genes (814 probes) were upregulated (>fivefold) in the activated state (supplemental online Table 2). We also examined the gene expression of proliferating satellite cells/myoblasts in vivo that were directly isolated from regenerating muscle 2 days after cardiotoxin injection. The activated and proliferating satellite cells in vivo showed an expression profile quite similar to satellite cells cultured in vitro (data not shown).

## Upregulation of Cell Cycle Regulators in Quiescent Satellite Cells

Under normal conditions, most satellite cells are in the G0 phase of the cell cycle, possibly preventing their premature exhaustion. It is of note that nine genes encoding negative regulators of the cell cycle were highly upregulated in the quiescent stage: *Rgs2* (*regulator of G-protein signaling 2*) (×69, ×23), *Rgs5* (×37, ×21), *Pmp22* (*peripheral myelin protein 22*)/*Gas3* (growth arrest specific 3) (×25), *Cdkn1c* (cyclin-dependent kinase inhibitor 1C)/*p57* (×14), *Spry1* (sprouty homolog 1) (×11), *Gas1* (×7, ×6), *Reck* (reversion-inducing-cysteine-rich protein with kazal motifs) (×6), *Ddit3* (DNA-damage inducible transcript 3) (×6), and *Trp63* (transformation-related protein 63) (×5) (supplemental online Table 1). Reverse transcription (RT)-PCR confirmed that *Rgs2*, *Pmp22*, *p57*, and *Spry1* are highly expressed in quiescent satellite cells and downregulated in activated satellite cells (Fig. 2Ba).

Cyclin-dependent kinase inhibitors (CKIs) play a key role in controlling the cell cycle in many cell types. p21 (CIP1) triggers the cell cycle exit of proliferating myoblasts to initiate myoblast terminal differentiation in response to differentiation signals [25]. p57 (KIP2) is induced in myoblasts upon differentiation. Gene targeting experiments showed that these two CKIs redundantly control cell cycle exit during myogenesis [26]. Compared with irreversible cell cycle arrest upon differentiation, however, attainment of a reversible G0 state by satellite cells is poorly understood. In vitro studies suggested that Rb family members p130 and p27 are involved in the reversible cell cycle exit of proliferating myoblasts to return satellite cells to quiescence [16]. In our experiments, p21 (×0.5), p27 (×1.5), and p130 (×2–3) were not significantly upregulated in quiescent satellite cells. Reflecting the levels of p57 mRNA, p57 protein was found in more than 90% of freshly isolated SM/C-2.6$^+$ cells (Fig. 2Ca). Whether p57 is required for acquisition and maintenance of quiescence of satellite cells remains to be determined in a future study.

## Upregulation of Myogenic Inhibitors in Quiescent Satellite Cells

Quiescent satellite cells barely express myogenic basic helix-loop-helix (bHLH) factors. Activity of the *Myf-5* locus was revealed through a reporter gene, but Myf-5 protein is hardly detected in dormant satellite cells. On activation, satellite cells upregulate Myf5 and start to express MyoD [27] (Fig. 1). Our microarray analyses revealed that several myogenic inhibitory molecules were upregulated in quiescent satellite cells: *Bmp6* (*bone morphogenetic protein 6*) (×214), *Bmp4* (×66), *Bmp2* (×82), *Heyl* (*hairy/enhancer-of-split related with YRPW motif-like*)/*Herp3*/*Hrt3*/*hesr3* (×101, ×33, ×32), *Musculin*/*MyoR* (×83), *Notch3* (×9). Upregulation of *Bmp4*, *Bmp6*, *Msc*/*MyoR*, and *Heyl* in quiescent satellite cells was confirmed by RT-PCR (Fig. 2Bb). BMP4 is reported to negatively regulate MyoD expression in somite myogenesis [28] and differentiation of satellite cells, where BMP4-induced inhibition of myogenic differentiation requires Notch signaling [29]. Notch signaling is reported to inhibit the differentiation of myoblasts by repression of MyoD expression [30]. In postnatal muscle, Notch signaling controls satellite cell activation and their cell fate [31], and insufficient upregulation of the Notch ligand Delta is casually related to impaired regeneration of aged muscle [32]. Among several molecules in the Notch signaling pathway, our microarray analysis showed that *Notch3* and one of the Notch-effector genes, *Heyl*, are highly expressed in quiescent satellite cells. When cross-sections of normal mouse tibialis anterior (TA) muscle were stained with specific antibodies, HeyL was found in nearly all Pax7-positive nuclei, and Notch3 was expressed on the surface of mononuclear cells beneath the basal lamina (Fig. 2Cb, 2Cc). These results suggest that Notch3 and HeyL play roles in Notch signaling to inhibit muscle differentiation of satellite cells. Musculin/MyoR is a bHLH transcription factor originally cloned as a repressor of MyoD [33]. Musculin-null mice do not exhibit any skeletal muscle defect, but musculin is likely to negatively regulate MyoD in muscle regeneration [34].

In addition to negative regulators, two positive regulators of myogenesis, *Gli2* (*GLI-Kruppel family member GLI2*) (×29, ×13) and *Meox2* (*mesenchyme homeobox 2*) (×17), are preferentially expressed in quiescent satellite cells. Gli2 directly upregulates Myf5 [35], and Meox1 and 2 regulate Pax3 and Pax7 expressions [36]. These observations suggest that Gli2 and Meox2 maintain lineage identity in quiescent satellite cells.

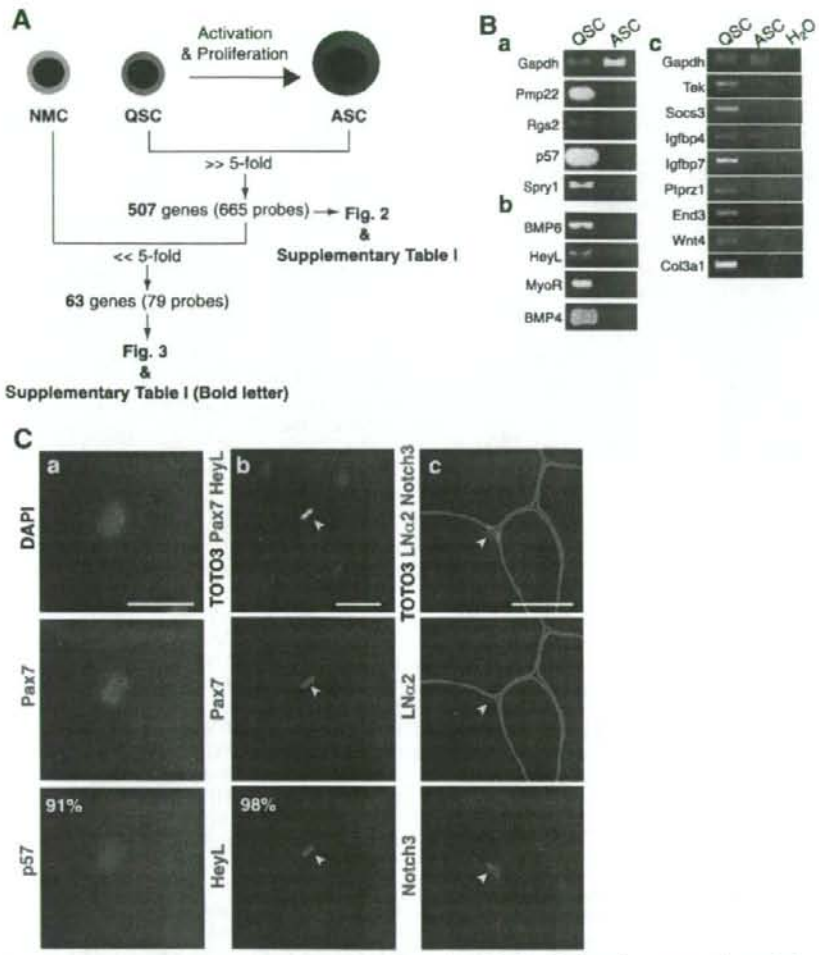


**Figure 2.** Identification of the genes expressed at higher levels in QSC than in ASC. **(A):** Outline of gene expression analysis at single gene level. Sixty-three genes out of 507 genes were found to be expressed at a higher level (more than fivefold) in quiescent satellite cells than in NMC. We applied Student's *t* test ($p$ value .05) with multiple testing corrections (Benjamini and Hochberg false discovery rate). **(B):** Reverse transcription-polymerase chain reaction of eight relevant genes involved in cell cycle regulation **(Ba)**, inhibition of myogenesis **(Bb)**, or other biological process **(Bc)** (Table 1). Total RNAs were isolated from fluorescence-activated cell sorting-sorted SM/C-2.6$^+$ cells (QSC) and cultured SM/C-2.6$^+$ cells (ASC). *Gapdh* is control. **(Ca):** Mononucleated cells from intact skeletal muscle were stained with anti-p57 (red), Pax7 (green), and DAPI (blue) immediately after sorting. **(Cb, Cc):** Cross-sections of normal skeletal muscle were stained with antibodies to HeyL (red in **[Cb]**), Notch3 (red in **[Cc]**), Pax7 (green in **[Cb]**), or laminin $\alpha$2 chain (green in **[Cc]**). More than 90% of Pax7-positive cells were positive for p57. Nearly all Pax7-positive cells expressed HeyL. Notch3 was expressed on the cell surface on satellite cells. Nuclei were stained with TOTO3 (blue). Scale bar: 20 $\mu$m. Abbreviations: ASC, activated satellite cells; DAPI, 4,6-diamidino-2-phenylindole; LN$\alpha$2, laminin $\alpha$2; NMC, nonmyogenic cells; QSC, quiescent satellite cells.

## Identification of Quiescent Satellite Cell-Specific Genes

To identify quiescent satellite cell-specific genes from 507 genes (Fig. 2A), we next prepared RNA samples from nonmyogenic cells (SM/C-2.6$^-$/CD45$^-$ in Fig. 1A) and performed microarray analysis using Affymetrix GeneChips. Statistical analysis validated that 63 genes out of 507 genes were preferentially expressed (>fivefold) in quiescent satellite cells compared with nonmyogenic cells or activated satellite cells (genes in bold letters in supplemental online Table 1).

To confirm the microarray results, we next performed RT-PCR on 14 genes of interest. In addition to microarray samples, the results for TA muscle and a myogenic cell line, C2C12 cells, are also shown (Fig. 3). Two well-established satellite cell markers (Pax7 and M-cadherin) were expressed not only in quiescent satellite cells but also in activated satellite cells and/or C2C12 cells. In contrast, two cell surface molecules, Odz4, a mouse homolog of the *Drosophila* pair-rule gene *Odd Oz* [37], and CTR, a signaling molecule Tribbles1, and two extracellular molecules, endothelin3 and chordin-like2, were all confirmed to be expressed exclusively in quiescent satellite cells.

## Gene Set Enrichment Analysis Revealed Gene Groups Upregulated in Quiescent Satellite Cells

Single-gene analysis permitted us to identify candidate genes that regulate quiescence and undifferentiated state of satellite cells in vivo. To complement the analysis at the single gene

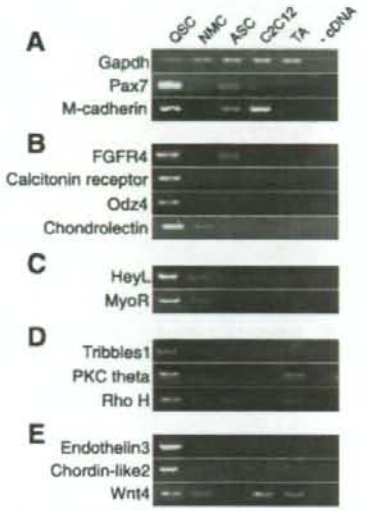


**Figure 3.** Reverse transcription-polymerase chain reaction (RT-PCR) of quiescent satellite cell-specific genes. Expression levels of quiescent satellite cell-specific genes in fluorescence-activated cell sorting-sorted SM/C-2.6$^+$ cells (lane 1), SM/C-2.6$^-$/CD45$^-$ non-myogenic cells (lane 2), cultured SM/C-2.6$^+$ cells (lane 3), C2C12 cells (lane 4), and TA muscle (lane 5) were confirmed by RT-PCR. The genes are categorized into five groups: well-known satellite cell markers (**A**), cell surface receptors (**B**), transcription factors (**C**), signal molecules (**D**), and extracellular molecules (**E**). Lane 6 is the reaction without cDNA templates. Abbreviations: ASC, activated satellite cells; NMC, nonmyogenic cells; QSC, quiescent satellite cells; TA, tibialis anterior.

level, we performed gene set enrichment analysis [22]. GSEA is an analytical method that identifies small but coordinated changes of predefined gene sets but not up- or downregulation of individual genes, which therefore would help us to identify important signaling pathways or regulatory mechanisms for satellite cells. We used GO annotations [23] to group all genes on GeneChips and tried to extract gene sets that are upregulated as a whole in quiescent satellite cells compared with activated and proliferating satellite cells (Fig. 4). When all genes were categorized into 1,674 gene sets according to their biological process ontology, only three gene sets were judged to be coordinately upregulated in quiescent satellite cells (FDR < 0.25): cell-cell adhesion, regulation of cell growth, and transmembrane receptor protein tyrosine phosphatase signaling pathway (Table 1). When all genes were grouped into 1,698 gene sets according to cellular component ontology, three gene sets, insoluble fraction, extracellular region, and collagens, were found to be coordinately upregulated in quiescent satellite cells compared with activated/proliferating satellite cells (Table 1). When grouped into 412 gene sets based on their predicted molecular functions, three gene sets, extracellular matrix structural constituent conferring tensile strength, copper ion binding, and lipid transporter activity, were found to be coordinately upregulated in quiescent satellite cells (Table 1). Seven genes listed in Table 1 (*Tek, Socs3, Igfbp7, Ptprz1, End3, Wnt4,* and *Col3a1*) were confirmed to be upregulated in quiescent satellite cells by RT-PCR (Fig. 2Bc). A more detailed discussion on GSEA results is in the supplemental online Discussion.

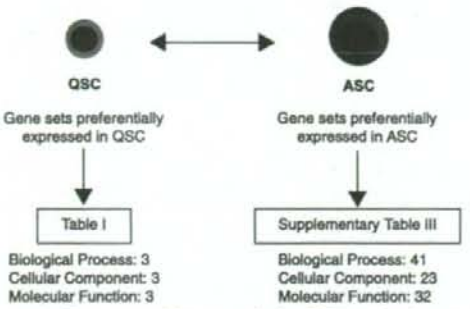


**Figure 4.** Gene set enrichment analysis (GSEA) of quiescent and activated satellite cells. Summary of GSEA comparing QSC with ASC using gene sets based on three major Gene Ontology trees: cellular component, biological process, and molecular function. Gene sets with high enrichment score (1 − [false discovery rate q value] are >0.75) are listed in Table 1 and supplemental online Table 3. Abbreviations: ASC, activated satellite cells; QSC, quiescent satellite cells.

## Gene Sets That Are Coordinately Upregulated upon Activation

Many gene sets were found to be coordinately upregulated in activated/proliferating satellite cells compared with quiescent satellite cells (Fig. 4). These are involved in active synthesis of DNA, RNA and protein, progression of cell cycle (*Cdc2a, Cdc20, Cdc25c, Ccnb1, Ccna2,* etc.), mitochondrial activities, and so on. The gene sets are all listed in supplemental online Table 3. The results well reflect active cell cycling and high metabolic activity of satellite cells.

## Expression of Cell-Cell Adhesion Molecules on Satellite Cells

Both single gene analysis and GSEA suggest that cell-cell adhesion is one of the key elements in the regulation of satellite cells. Preferential expression of the following genes in quiescent satellite cells was confirmed by RT-PCR and quantitative PCR (supplemental online Fig. 1A, 1B): *VE-cadherin* (*cadherin 5*), *Vcam1, Icam1, Cldn5* (*claudin 5*), *Esam* (*endothelial cell-specific adhesion molecule*), and *Pcdhb9* (*protocadherin beta 9*). To date, several cell surface markers for satellite cells have been identified, including M-cadherin, syndecan3, syndecan4, c-met, Vcam-1, NCAM-1, and CD34 [5, 38–43]. Vascular endothelial (VE)-cadherin, Icam1, claudin5, Esam, and Pcdhb9 should be added to the list. Because *Esam* is upregulated in long-term hematopoietic stem cells and mammary gland side population cells [44, 45], the expression of *Esam* in quiescent satellite cells is quite intriguing. When transverse sections of adult skeletal muscle were stained with specific antibodies, M-cadherin was found at the site of contact between satellite cells and myofibers (supplemental online Fig. 1C) [38]. Vcam-1 and VE-cadherin proteins are also detected at the boundary of satellite cells and myofibers. Although their roles in regulation of satellite cells remain to be determined, our observations suggest that cell-cell adhesion molecules have critical roles in keeping satellite cells in an undifferentiated and quiescent state and in protecting satellite cells from cell death. We also confirmed that FACS with Vcam-1 anti-

**Table 1.** Gene sets upregulated in quiescent satellite cells and genes with high enrichment scores

| | 1 − (FDR q value) |
|---|---|
| Biological process | |
| Cell-cell adhesion | .791 |
| *Tek, Vcam1, Icam2, Cldn5, Cdh5, Icam1* | |
| Regulation of cell growth | .787 |
| *Socs3, Htra1, Htra3, Ctgf, Igfbp4, Creg1, Igfbp7, Epc1, Cyr61, Crim1, Nov, Igfbp6, Nedd9* | |
| Transmembrane receptor protein tyrosine phosphatase signaling pathway | .751 |
| *Ptprz1, Ptprf, Ptprb, Ptprd, Ptprk, Ptprs, Ptprr* | |
| Cellular component | |
| Insoluble fraction | .786 |
| *Dmd, Dag1, Plec1, Des, Hspb1* | |
| Extracellular region | .766 |
| *Sepp1, Htra1, Edn3, Cxcl1, Loxl1, Htra3, Thbs4, Ctgf, Ntf3, Twsg1, Ccl27, Rarres2, Ltbp3, Igfbp4, Apoe, Igf1, Ibsp, Trf, Pthlh, Polydom, Ccl11, Abca3, Thbs3, Wnt4, Pros1, Vwa1, Comp, Nppc, Cyp4v3, Ccl19, Nts, Fbln2, Cocoacrisp, Cxcl2, Igfbp7, C1r, Thbs2, Ccl6, Calca, Cyr61, Icosl, Ccl21c, Crim1, Il6, Degb10, Cxcl9, Csng, C3, Cxcl10, Cxcl14, Inhbb, Il15, Nov, Igfbp6, Mglap, Dkk2, Tnfsf12, Ifnb1, Tfpi2, Cxcl11, Il18, Pi16, Pycard, Lzp-s, Stc1, Lyzs* | |
| Collagen | .766 |
| *Col3a1, Col6a2, Col17a1, Col1a2, Col15a1, Col6a3, Col5a3, Col1a1, Col4a1, Col5a1, Col11a1* | |
| Molecular function | |
| Extracellular matrix structural constituents conferring tensile strength | .774 |
| *Col3a1, Col6a2, Col17a1, Col1a2, Col15a1, Col6a3, Col16a1, Col1a1, Col4a1, Col4a5, Col5a1, Col11a1, Col11a2, Col9a1, Col4a2, Col4a4* | |
| Copper ion binding | .764 |
| *Aoc3, Cp, Loxl1, Mt1, Atp7a, Heph, Loxl2, Nr1h3* | |
| Lipid transporter activity | .752 |
| *Vldlr, Lp1, Apoe, Sorl1, Ldlr, Gpld1, Lrp1* | |

Gene names are listed according to the rank of enrichment scores. Underlined genes (46/118 genes) are also listed in supplemental online Table 1.
Abbreviation: FDR, false discovery rate.

body efficiently enriches quiescent satellite cells as SM/C-2.6 does (supplemental online Fig. 2).

## Calcitonin Receptor Is Sharply Downregulated on Activated Satellite Cells and Reappeared on Renewed Satellite Cells During Muscle Regeneration

RT-PCR verified that CTR is exclusively expressed in quiescent satellite cells but not in activated satellite cells or in nonmyogenic cells (Fig. 3). In addition, we confirmed that calcitonin mRNA is expressed in satellite cells (data not shown). Therefore, we examined the expression of CTR protein in vivo using immunohistochemistry. As shown in Figure 5A, CTR protein was observed in Pax7-positive mononuclear cells beneath the basal lamina in uninjured muscle. We next stained cross-sections of regenerating muscle with anti-CTR antibody. Three days after cardiotoxin injection, many activated satellite cells were stained with anti-M-cadherin antibodies, but CTR expression was not detected on activated satellite cells on the serial sections (Fig. 5B). Furthermore, there were no $Pax7^+/CTR^+$ cells on muscle sections until 7 days after injury (cardiotoxin [CTX]-7d), when $Pax7^+/CTR^+$ cells were again found at the periphery of centrally nucleated, relatively large myofibers but not of small regenerating fibers (Fig. 5C, 5D). The number of $Pax7^+/CTR^+$ cells gradually increased thereafter and reached the level of uninjured muscle by CTX-14d (Fig. 5D). Interestingly, approximately 20% of $Pax7^+/CTR^+$ cells on CTX-7d were found outside the basal lamina (Fig. 5E). This atypical position of satellite cells was transient, and the ratio of satellite cells residing beneath the basal lamina increased during myofiber maturation (data not shown). Taken together, the results suggest that the expression of CTR is found not only on quiescent satellite cells but also on newly formed satellite cells that are closely associated with maturing myofibers.

## Calcitonin Inhibits Activation of Quiescent Satellite Cells

To investigate the roles of CTR in the regulation of satellite cells, eel calcitonin, elcatonin, was added to the culture of quiescent satellite cells in vitro before or after activation. Addition of calcitonin before activation significantly inhibited BrdU uptake by quiescent satellite cells (Fig. 6A) but not by already activated satellite cells (Fig. 6A). Interestingly, a short exposure (0.5 hours) to calcitonin was enough to suppress the activation of quiescent satellite cells (Fig. 6B).

MyoD staining of satellite cells revealed that calcitonin/CTR signaling delays the induction of MyoD in quiescent satellite cells (Fig. 6C). The lower percentage of Ki67-positive cells in calcitonin-treated satellite cells also indicated that calcitonin delays the entry of quiescent satellite cells into the cell cycle (Fig. 6C). Calcitonin-treated cells were considerably smaller than control cells on the second day of culture (Fig. 6D), again indicating delayed activation of satellite cells in the presence of calcitonin. A terminal deoxynucleotidyl transferase dUTP nick-end labeling assay excludes the possibility that calcitonin induced apoptosis in satellite cells (Fig. 6E).

To further investigate the effects of calcitonin on activation of quiescent satellite cells, we prepared living single muscle fibers from mouse extensor digitorum longus muscles by using the collagenase digestion method [20] and plated them onto Matrigel-coated 24-well plates at a density of one fiber per well in the presence or absence of calcitonin. In control wells, many satellite cells had detached and migrated from the myofibers 2 days after plating (Fig. 6F). Calcitonin significantly reduced the numbers of satellite cells that had detached from myofibers (Fig. 6F). It was reported that

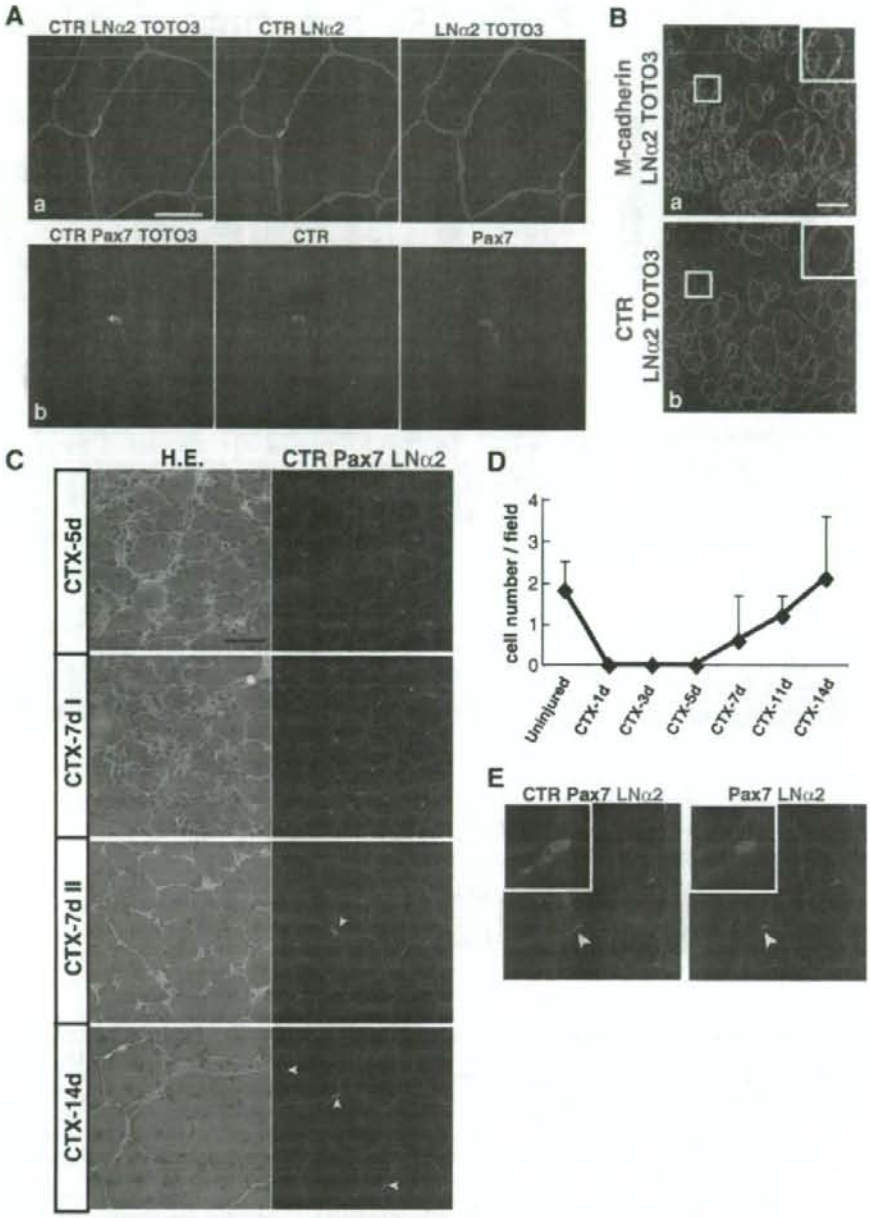


**Figure 5.** Reappearance of CTR- and Pax7-positive satellite cells in regenerating muscle 7 days after cardiotoxin injection. **(A):** Cross-sections of uninjured skeletal muscle were stained with antibodies to calcitonin receptor (red), laminin $\alpha 2$ chain (green in [Aa]), or Pax7 (green in [Ab]). Nuclei were stained with TOTO3 (blue). Scale bar: 20 $\mu$m. **(B):** Three days after CTX injection, regenerating muscles were dissected, and serial cross-sections were stained with antibodies to M-cadherin (red in **[Ba]**) or CTR (red in **[Bb]**) and anti-laminin $\alpha 2$ (green in **[Ba, Bb]**) antibodies. Insets show close-ups of marked areas by white squares. Nuclei were stained with TOTO3 (blue). Scale bar: 40 $\mu$m. **(C):** Tibialis anterior muscles were sampled at five (CTX-5d), seven (CTX-7d), and 14 days (CTX-14d) after CTX injection. Sections were coimmunostained with anti-CTR (red), Pax7 (green), and laminin $\alpha 2$ chain (blue) antibodies. Serial sections were stained with H.E. Note that $Pax7^+/CTR^+$ cells were first detected on the seventh day of regeneration around regenerating muscle fibers with a large diameter (CTX-7d II) but not around small-sized fibers (CTX-7d I). Arrowheads indicate CTR-positive Pax7-positive cells. Scale bar: 40 $\mu$m. **(D):** Numbers of $Pax7^+/CTR^+$ cells per field at 1, 3, 5, 7, 11, and 14 days after CTX injection. $Pax7^+/CTR^+$ cells were counted in 12–21 randomly selected fields in the regenerating area. The average is shown with SD. **(E):** Cross-sections of regenerating muscle 7 days after CTX injection were coimmunostained with CTR (red), Pax7 (green), and laminin $\alpha 2$ (blue). A typical $Pax7^+/CTR^+$ satellite cell outside the basal lamina is shown (arrowheads). Scale bar: 20 $\mu$m. Abbreviations: CTR, calcitonin receptor; CTX, cardiotoxin; d, day; H.E., hematoxylin and eosin; LN$\alpha 2$, laminin $\alpha 2$.

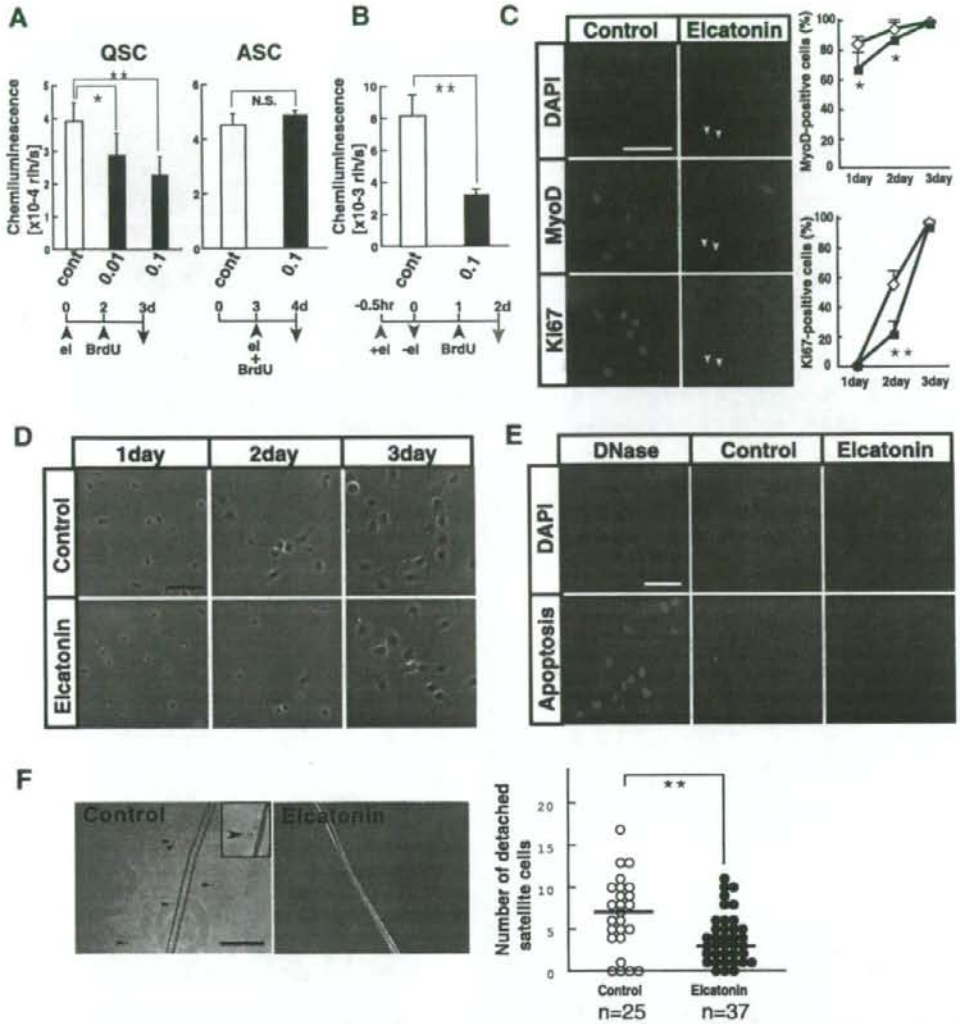


**Figure 6.** Calcitonin receptor agonist, elcatonin, suppresses activation of quiescent satellite cells. **(A):** Freshly isolated SM/C-2.6$^+$ cells (QSC) and cultured SM/C-2.6$^+$ cells (ASC) were grown in the presence (black) or absence (white) of eel calcitonin, elcatonin. Left: QSC were cultured for 2 days with (0.01 U/ml or 0.1 U/ml) or without elcatonin and then cultured for an additional 24 hours in the presence of BrdU. Right: QSC were cultured for 3 days and then cultured for 24 hours in the presence or absence of elcatonin and BrdU. The vertical axis shows the mean BrdU uptake by satellite cells of three experiments with SD; * $p < .05$, ** $p < .01$ (analysis of variance [ANOVA] test). **(B):** BrdU uptake by QSC exposed to elcatonin for 30 minutes prior to plating. Values are means with SD ($n = 3$); ** $p < .01$. **(C):** QSC cultured in the presence or absence of 0.1 U/ml elcatonin for 2 days were stained with anti-MyoD (red) or Ki67 (green) antibodies. Nuclei were stained with DAPI (blue). Arrowheads indicate MyoD- and Ki67-negative satellite cells. Graphs show the frequency of MyoD- or Ki67-positive cells 1, 2, or 3 days after plating with (closed square) or without (open diamond) elcatonin. More than 100 cells were counted. Values are means with SD; * $p < .05$, ** $p < .01$. Scale bar: 50 $\mu$m. **(D):** Phase contrast images of satellite cells 1, 2, and 3 days after plating in the presence or absence of 0.1 U/ml elcatonin. Note that many elcatonin-treated satellite cells are smaller than nontreated cells 2 days after plating. Scale bar: 50 $\mu$m. **(E):** Terminal deoxynucleotidyl transferase dUTP nick-end labeling assay on satellite cells cultured with or without elcatonin for 2 days. Apoptotic cells are in red. Nuclei were stained with DAPI (blue). As a positive control, satellite cells were pretreated with DNase. Scale bar: 50 $\mu$m. **(F):** Activation of satellite cells on myofibers in vitro. Isolated muscle fibers were plated at a density of one fiber per well and cultured with or without elcatonin (0.1 U/ml) for 2 days, and the numbers of satellite cells that had detached and migrated from each muscle fiber (arrowheads) were counted. Inset is a close-up image of a detached satellite cell. Scale bar: 100 $\mu$m. ANOVA $t$ test, ** $p < .01$. Abbreviations: ASC, activated satellite cells; BrdU, 5-bromo-2′-deoxyuridine; d, days; DAPI, 4,6-diamidino-2-phenylindole; el, elcatonin; hr, hours; NS, nonsignificant; QSC, quiescent satellite cells.

calcitonin signaling was mediated via cAMP [46]. An analog of cAMP, dibutyryl cAMP, and an activator of adenylate cyclase, forskolin, also attenuated the activation of satellite cells in vitro (data not shown). Collectively, our results suggest that calcitonin/CTR signaling inhibits activation of satellite cells but not their proliferation or survival. The downstream target molecules of calcitonin/CTR remain to be determined.

## CONCLUSION

Single gene-level analysis revealed several candidate genes that negatively regulate cell cycling of satellite cells. Furthermore, our results suggested that satellite cells express both myogenic and antimyogenic molecules to maintain their delicate state.

GSEA showed that dormant satellite cells coordinately express gene groups involved in cell-cell adhesion, cell-extracellular matrix interaction, copper and iron homeostasis, lipid transport, and regulation of cell growth. Although the result shows one aspect of regulation of quiescent satellite cells, more elaborate gene grouping might be needed to further understand the molecular regulation of quiescent satellite cells.

Finally, we showed that calcitonin receptor is specifically expressed on quiescent satellite cells and transmits signals that attenuate the entry of quiescent satellite cells into the cell cycle. Our results would greatly facilitate the investigation of molecular regulation of satellite cells in both physiological and pathological conditions.

## ACKNOWLEDGMENTS

This work was supported by Grants for Research on Nervous and Mental Disorders (16B-2), Health Science Research Grants for Research on the Human Genome and Gene Therapy (H16-genome-003), for Research on Brain Science (H15-Brain-021) from the Japanese Ministry of Health, Labor and Welfare, Grants-in-Aids for Scientific Research (14657158, 153,90281, and 165,90333) from the Japanese Ministry of Education, Culture, Sports, Science and Technology, and "Ground-Based Research Program for Space Utilization" promoted by Japan Space Forum.

## DISCLOSURE OF POTENTIAL CONFLICTS OF INTEREST

The authors indicate no potential conflicts of interest.

## REFERENCES

1 Bischoff R. Analysis of muscle regeneration using single myofibers in culture. Med Sci Sports Exerc 1989;21(suppl 5):S164–S172.
2 Partridge T. Reenthronement of the muscle satellite cell. Cell 2004;119: 447–448.
3 Mauro A. Satellite cell of skeletal muscle fibers. J Biophys Biochem Cytol 1961;9:493–495.
4 Schultz E, Gibson MC, Champion T. Satellite cells are mitotically quiescent in mature mouse muscle: an EM and radioautographic study. J Exp Zool 1978;206:451–456.
5 Cornelison DD, Wold BJ. Single-cell analysis of regulatory gene expression in quiescent and activated mouse skeletal muscle satellite cells. Dev Biol 1997;191:270–283.
6 Bischoff R. Satellite and stem cells in muscle regeneration. In: Engel AG, Franzini-Armstrong C, eds. Myology. Vol 1. New York: McGraw-Hill, 2004:66–86.
7 Collins CA, Olsen I, Zammit PS et al. Stem cell function, self-renewal, and behavioral heterogeneity of cells from the adult muscle satellite cell niche. Cell 2005;122:289–301.
8 Seale P, Sabourin LA, Girgis-Gabardo A et al. Pax7 is required for the specification of myogenic satellite cells. Cell 2000;102:777–786.
9 Grounds MD, Yablonka-Reuveni Z. Molecular and cell biology of skeletal muscle regeneration. Mol Cell Biol Hum Dis Ser 1993;3: 210–256.
10 Wagers AJ, Conboy IM. Cellular and molecular signatures of muscle regeneration: Current concepts and controversies in adult myogenesis. Cell 2005;122:659–667.
11 Asakura A, Komaki M, Rudnicki M. Muscle satellite cells are multipotential stem cells that exhibit myogenic, osteogenic, and adipogenic differentiation. Differentiation 2001;68:245–253.
12 Wada MR, Inagawa-Ogashiwa M, Shimizu S et al. Generation of different fates from multipotent muscle stem cells. Development 2002;129: 2987–2995.
13 Shefer G, Wleklinski-Lee M, Yablonka-Reuveni Z. Skeletal muscle satellite cells can spontaneously enter an alternative mesenchymal pathway. J Cell Sci 2004;117:5393–5404.
14 McCroskery S, Thomas M, Maxwell L et al. Myostatin negatively regulates satellite cell activation and self-renewal. J Cell Biol 2003;162: 1135–1147.
15 Thomas M, Langley B, Berry C et al. Myostatin, a negative regulator of muscle growth, functions by inhibiting myoblast proliferation. J Biol Chem 2000;275:40235–40243.
16 Cao Y, Zhao Z, Gruszczynska-Biegala J et al. Role of metalloprotease disintegrin ADAM12 in determination of quiescent reserve cells during myogenic differentiation in vitro. Mol Cell Biol 2003;23: 6725–6738.
17 Carnac G, Fajas L, L'Honore A et al. The retinoblastoma-like protein p130 is involved in the determination of reserve cells in differentiating myoblasts. Curr Biol 2000;10:543–546.
18 Fukada S, Higuchi S, Segawa M et al. Purification and cell-surface marker characterization of quiescent satellite cells from murine skeletal muscle by a novel monoclonal antibody. Exp Cell Res 2004;296: 245–255.
19 Uezumi A, Ojima K, Fukada S et al. Functional heterogeneity of side population cells in skeletal muscle. Biochem Biophys Res Commun 2006;341:864–873.
20 Rosenblatt JD, Lunt AI, Parry DJ et al. Culturing satellite cells from living single muscle fiber explants. In Vitro Cell Dev Biol Anim 1995; 31:773–779.
21 Ojima K, Uezumi A, Miyoshi H et al. Mac-1(low) early myeloid cells in the bone marrow-derived SP fraction migrate into injured skeletal muscle and participate in muscle regeneration. Biochem Biophys Res Commun 2004;321:1050–1061.
22 Mootha VK, Lindgren CM, Eriksson KF et al. PGC-1alpha-responsive genes involved in oxidative phosphorylation are coordinately downregulated in human diabetes. Nat Genet 2003;34:267–273.
23 Ashburner M, Ball CA, Blake JA et al. Gene ontology: Tool for the unification of biology. The Gene Ontology Consortium. Nat Genet 2000;25:25–29.
24 Holyoake T, Jiang X, Eaves C et al. Isolation of a highly quiescent subpopulation of primitive leukemic cells in chronic myeloid leukemia. Blood 1999;94:2056–2064.
25 Missero C, Calautti E, Eckner R et al. Involvement of the cell-cycle inhibitor Cip1/WAF1 and the E1A-associated p300 protein in terminal differentiation. Proc Natl Acad Sci U S A 1995;92:5451–5455.
26 Zhang P, Wong C, Liu D et al. p21(CIP1) and p57(KIP2) control muscle differentiation at the myogenin step. Genes Dev 1999;13:213–224.
27 Cooper RN, Tajbakhsh S, Mouly V et al. In vivo satellite cell activation via Myf5 and MyoD in regenerating mouse skeletal muscle. J Cell Sci 1999;112:2895–2901.
28 Reshef R, Maroto M, Lassar AB. Regulation of dorsal somitic cell fates: BMPs and Noggin control the timing and pattern of myogenic regulator expression. Genes Dev 1998;12:290–303.
29 Dahlqvist C, Blokzijl A, Chapman G et al. Functional Notch signaling is required for BMP4-induced inhibition of myogenic differentiation. Development 2003;130:6089–6099.
30 Kuroda K, Tani S, Tamura K et al. Delta-induced Notch signaling mediated by RBP-J inhibits MyoD expression and myogenesis. J Biol Chem 1999;274:7238–7244.
31 Conboy IM, Rando TA. The regulation of Notch signaling controls satellite cell activation and cell fate determination in postnatal myogenesis. Dev Cell 2002;3:397–409.
32 Conboy IM, Conboy MJ, Smythe GM et al. Notch-mediated restoration of regenerative potential to aged muscle. Science 2003;302: 1575–1577.
33 Lu J, Webb R, Richardson JA et al. MyoR: A muscle-restricted basic helix-loop-helix transcription factor that antagonizes the actions of MyoD. Proc Natl Acad Sci U S A 1999;96:552–557.
34 Zhao P, Hoffman EP. Musculin isoforms and repression of MyoD in muscle regeneration. Biochem Biophys Res Commun 2006;342: 835–842.
35 Gustafsson MK, Pan H, Pinney DF et al. Myf5 is a direct target of long-range Shh signaling and Gli regulation for muscle specification. Genes Dev 2002;16:114–126.
36 Mankoo BS, Skuntz S, Harrigan I et al. The concerted action of Meox homeobox genes is required upstream of genetic pathways essential for the formation, patterning and differentiation of somites. Development 2003;130:4655–4664.

37 Zhou XH, Brandau O, Feng K et al. The murine Ten-m/Odz genes show distinct but overlapping expression patterns during development and in adult brain. Gene Expr Patterns 2003;3:397–405.
38 Irintchev A, Zeschnigk M, Starzinski-Powitz A et al. Expression pattern of M-cadherin in normal, denervated, and regenerating mouse muscles. Dev Dyn 1994;199:326–337.
39 Cornelison DD, Filla MS, Stanley HM et al. Syndecan-3 and syndecan-4 specifically mark skeletal muscle satellite cells and are implicated in satellite cell maintenance and muscle regeneration. Dev Biol 2001;239: 79–94.
40 Beauchamp JR, Heslop L, Yu DS et al. Expression of CD34 and Myf5 defines the majority of quiescent adult skeletal muscle satellite cells. J Cell Biol 2000;151:1221–1234.
41 Jesse TL, LaChance R, Iademarco MF et al. Interferon regulatory factor-2 is a transcriptional activator in muscle where It regulates expression of vascular cell adhesion molecule-1. J Cell Biol 1998; 140:1265–1276.
42 Illa I, Leon-Monzon M, Dalakas MC. Regenerating and denervated human muscle fibers and satellite cells express neural cell adhesion molecule recognized by monoclonal antibodies to natural killer cells. Ann Neurol 1992;31:46–52.
43 Charge SB, Rudnicki MA. Cellular and molecular regulation of muscle regeneration. Physiol Rev 2004;84:209–238.
44 Forsberg EC, Prohaska SS, Katzman S et al. Differential expression of novel potential regulators in hematopoietic stem cells. PLoS Genet 2005;1:e28.
45 Behbod F, Xian W, Shaw CA et al. Transcriptional profiling of mammary gland side population cells. STEM CELLS 2006;24:1065–1074.
46 Becker K, Muller B, Nylen E et al. Calcitonin Gene Family of Peptides. Vol 1. 2nd ed. New York: Academic Press, 2002.

See www.StemCells.com for supplemental material available online.

Gene Therapy (2007) 14, 1249–1260

www.nature.com/gt

ORIGINAL ARTICLE

# Injection of a recombinant AAV serotype 2 into canine skeletal muscles evokes strong immune responses against transgene products

K Yuasa[1,2], M Yoshimura[1], N Urasawa[1], S Ohshima[1], JM Howell[3], A Nakamura[1], T Hijikata[2], Y Miyagoe-Suzuki[1] and S Takeda[1]

[1]Department of Molecular Therapy, National Institute of Neuroscience, National Center of Neurology and Psychiatry, Kodaira, Tokyo, Japan; [2]Research Institute of Pharmaceutical Sciences, Faculty of Pharmacy, Musashino University, Nishi-tokyo, Tokyo, Japan and [3]Division of Veterinary and Biomedical Sciences, Murdoch University, Perth, Western Australia, Australia

*Using murine models, we have previously demonstrated that recombinant adeno-associated virus (rAAV)-mediated microdystrophin gene transfer is a promising approach to treatment of Duchenne muscular dystrophy (DMD). To examine further therapeutic effects and the safety issue of rAAV-mediated microdystrophin gene transfer using larger animal models, such as dystrophic dog models, we first investigated transduction efficiency of rAAV in wild-type canine muscle cells, and found that rAAV2 encoding β-galactosidase effectively transduces canine primary myotubes in vitro. Subsequent rAAV2 transfer into skeletal muscles of normal dogs, however, resulted in low and transient expression of β-galactosidase together with intense cellular infiltrations in vivo, where cellular and humoral immune responses were remarkably activated. In contrast, rAAV2 expressing no transgene elicited no cellular infiltrations. Co-administration of immunosuppressants, cyclosporine and mycophenolate mofetil could partially improve rAAV2 transduction. Collectively, these results suggest that immune responses against the transgene product caused cellular infiltration and eliminated transduced myofibers in dogs. Furthermore, in vitro interferon-γ release assay showed that canine splenocytes respond to immunogens or mitogens more susceptibly than murine ones. Our results emphasize the importance to scrutinize the immune responses to AAV vectors in larger animal models before applying rAAV-mediated gene therapy to DMD patients.*

Gene Therapy (2007) **14**, 1249–1260; doi:10.1038/sj.gt.3302984; published online 21 June 2007

**Keywords:** *AAV; gene transfer; skeletal muscle; dog; immune response; Duchenne muscular dystrophy*

## Introduction

Duchenne muscular dystrophy (DMD) is an X-linked, lethal disorder of skeletal muscle caused by mutations in the dystrophin gene, which encodes a large subsarcolemmal cytoskeletal protein, dystrophin. DMD is characterized by a high incidence (one among 3500 boys) and a high frequency of *de novo* mutation.[1] The absence of dystrophin accompanies the loss of dystrophin-associated glycoprotein complex from the sarcolemma and results in progressive muscle weakness, cardiomyopathy and early death. Although several treatment modalities, such as gene, cell and pharmacological therapies, have been researched to aim at correcting the dystrophic phenotypes, DMD currently has no effective treatment.

An adeno-associated virus (AAV) vector is a potential tool for gene therapy of inherited neuromuscular disorders. It is a nonpathogenic, low immunogenic and replication-defective viral vector that effectively infect nondividing cells, such as skeletal muscle fibers.[2] The size of exogenous DNA fragment which can be inserted into recombinant AAV vectors (rAAVs), however, is limited to up to 4.9 kb. Therefore, full-length dystrophin (14 kb) and mini-dystrophin (6.4 kb) cDNAs are too large to be incorporated into a rAAV. We and others have tried to design a short but functional microdystrophin gene that could be utilized as the therapeutic tool for DMD.[3–6] We constructed a series of rod-truncated microdystrophin cDNAs,[3] and generated transgenic *mdx* mice expressing each microdystrophin, and demonstrated that microdystrophin CS1 with four rod repeats and three hinges was a good candidate for therapeutic molecule.[7] We have also showed that the muscle-specific muscle creatine kinase (MCK) promoter in a rAAV drives longer transgene expression than the ubiquitous cytomegalovirus (CMV) promoter in *mdx* muscle.[8] Therefore, we generated the rAAV2 expressing microdystrophin ΔCS1 (3.8 kb cDNA) driven by the MCK promoter and introduced it into *mdx* muscles, and showed that sustained expression of microdystrophin from rAAV significantly ameliorates dystrophic phenotypes of

Correspondence: Dr S Takeda, Department of Molecular Therapy, National Institute of Neuroscience, National Center of Neurology and Psychiatry, 4-1-1 Ogawa-higashi, Kodaira, Tokyo 187-8502, Japan.
E-mail: takeda@ncnp.go.jp
Received 8 October 2006; revised 3 April 2007; accepted 14 May 2007; published online 21 June 2007

treated *mdx* mice.[9] These results indicate that rAAV-mediated microdystrophin transfer is a good therapeutic strategy for dystrophin deficiency.

For the application of our strategy to DMD patients, it is necessary to examine the therapeutic effects and the safety issue in larger animal models. To this end, we have recently established a colony of beagle-based canine X-linked muscular dystrophy in Japan ($CXMD_J$).[10,11] In contrast to moderate dystrophic changes of *mdx* mice, $CXMD_J$ show similar dystrophic phenotypes to those of human DMD: increased serum creatine kinase level, gross muscle atrophy with joint contractures, cardiomyopathy, prominent muscle necrosis, degeneration with mineralization and concurrent regeneration, and endomysial and perimysial fibrosis.[11,12] Therefore, affected dogs are useful for preclinical trials to predict the clinical effectiveness in DMD application. In addition, side effects of treatment modalities should be investigated in detail in the dog model to avoid unexpected, detrimental effects on DMD patients. For instance, human trial in hemophilia B was ineffective due to T-cell-mediated immunity to AAV capsid antigens, and represented the matter that further studies for immunomodulation in preclinical and human trials were required to achieve successful transduction.[13]

In this report, we demonstrate that rAAV2 efficiently infect canine myotubes and express the *lacZ* gene *in vitro*. In contrast, rAAV-mediated gene transfer into canine muscle *in vivo* elicits severe immune responses against the gene product, due to susceptive immune responses in the dog. These results suggest that it is important to know molecular backgrounds of immune response against AAV particles and its gene product in the host and consider immunosuppression in preclinical and clinical settings.

## Results

### *rAAV2-CMVLacZ efficiently transduces canine primary myotubes* in vitro

To investigate the transduction efficiency of a rAAV2 in canine muscle cells, we first infected primary myotubes prepared from C57BL/6 mice and wild-type beagle with rAAV type 2 encoding β-galactosidase (β-gal) driven by the CMV promoter (rAAV2-CMVLacZ) at doses from $2 \times 10^8$ to $2 \times 10^{11}$ vector genomes (vg) (Figure 1). Surprisingly, more canine myotubes were β-gal-positive than murine ones. To enhance the transgene expression by converting single-strand viral DNAs into double-strand DNAs after the rAAV infection,[14] we next co-infected myotubes with helper adenovirus (Ad) and rAAV2. As expected, Ad enhanced the expression of *lacZ* in both murine and canine myotubes, but β-gal expression was much more robust in canine primary myotubes than in mouse primary myotubes.

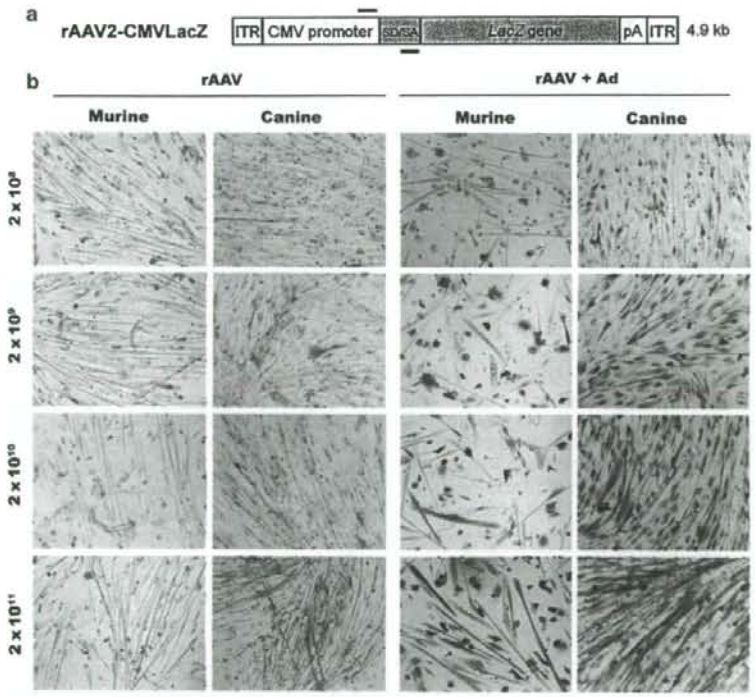


**Figure 1** Successful transduction of a rAAV2 in murine or canine primary myotubes *in vitro*. (a) Diagram of rAAV2-CMVLacZ. Upper and lower bars correspond to primer positions used for detection of genome and mRNA in Figure 2b. SD/SA: splicing donor and acceptor. (b) *In vitro* infection assay of rAAV2-CMVLacZ in murine and canine primary myotubes. Myotubes were infected with serial doses ($2 \times 10^8$–$2 \times 10^{11}$ vg/well) of rAAV2-CMVLacZ in the absence or presence of adenovirus (+Ad), and 2 days later β-gal expression was detected by X-Gal staining. Magnification: ×400. β-gal, β-galactosidase; X-Gal, 5-bromo-4-chloro-3-indolyl-β-D-galactopyranoside.

### *Low efficacy of gene transfer via rAAV into canine skeletal muscle* in vivo

To examine the transduction efficiency of rAAV2 in canine myofibers *in vivo*, rAAV2-CMVLacZ was injected into skeletal muscles of wild-type beagles and golden retrievers at various ages, and $\beta$-gal expression in the rAAV-injected muscles were evaluated at 2, 4 and 8 weeks after the injection (Figure 2a and Table 1). We previously reported that intramuscular injection of the rAAV2 into normal mice permitted sustained $\beta$-gal expression for at least 8 weeks.[8] In contrast to the mice, however, a few $\beta$-gal-positive fibers were observed in canine muscles at 2, 4 and 8 weeks after the injection of rAAV2-CMVLacZ both in beagles and golden retrievers. Moreover, in the rAAV2-injected canine muscles, a large number of mononuclear cells were observed around $\beta$-gal-expressing fibers at 2, 4 and 8 weeks after the injection (hematoxylin and eosin (H&E) in Figure 2a, Table 1). rAAV injection at neonatal stage or administration of low dose of the rAAV resulted in a little prolonged

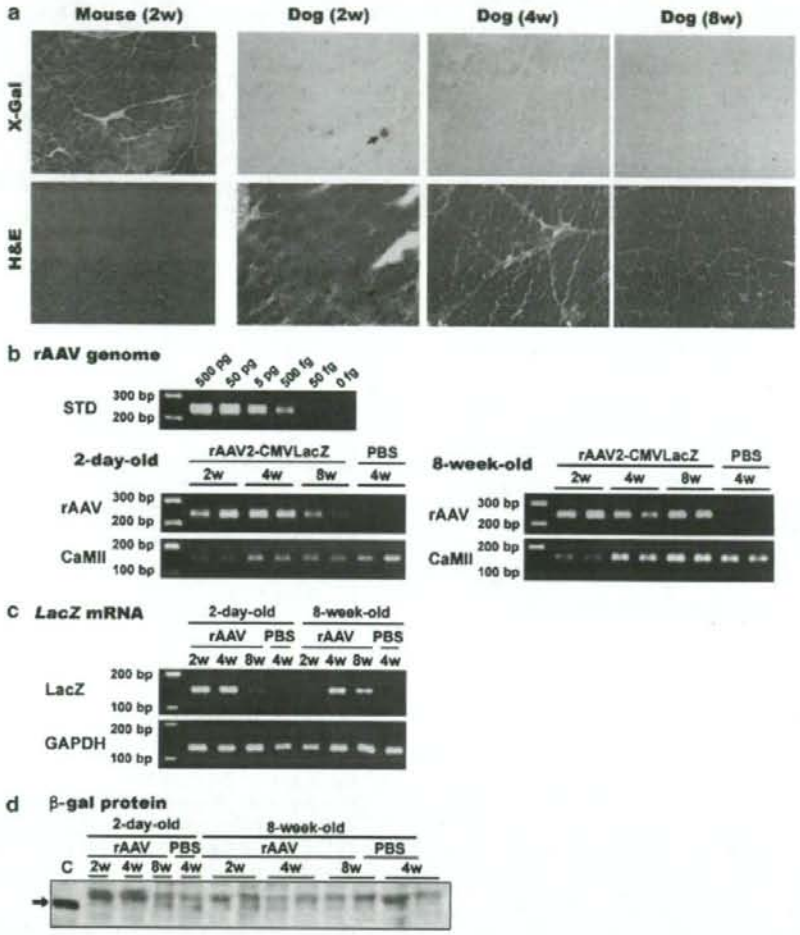


**Figure 2** Low transgene expression and marked cellular infiltration after rAAV2-mediated gene transfer into canine skeletal muscle. rAAV2-CMVLacZ was injected into normal muscles of beagles or golden retrievers at various ages. (**a**) Representative images of $\beta$-gal expression and histological change in the rAAV-injected murine (TA) and canine muscles at 2, 4 and 8 weeks post-injection (left TA, right TA and right ECU muscles of dog FD89 in Table 1, respectively). The same batches of rAAV2-CMVLacZ were injected into murine and canine skeletal muscles. Identical parts of the serial cross-sections were shown in X-Gal and H&E stains. Large and widespread (2w), or scattered clusters (4w, 8w) of infiltrating cells were observed in the rAAV-injected canine muscles. Magnification: $\times$200. (**b**, **c** and **d**) Detection of rAAV genomes (**b**), transgene mRNA (**c**) and $\beta$-gal protein (**d**) in the canine muscles injected at 2 days (dogs: 3290 and 0665) and 8 weeks (dogs: 0338). Total DNA, RNA or protein was extracted from rAAV2-CMVLacZ- or PBS-injected muscles after 2, 4 and 8 weeks post-injection. Genome (244 bp) or mRNA sequences (178 bp) of the rAAV was amplified from 200 ng of template DNA or an aliquot of RNA by PCR or RT-PCR, respectively (**b**, **c**). STD: quantity standard of AAV vector plasmid; rAAV: rAAV2-CMVLacZ genome; LacZ: $\beta$-gal mRNA; CaMII and GAPDH: internal controls of genome and message. Muscle extracts (40 $\mu$g/lane) and control $\beta$-gal (lane c) were separated on a sodium dodecyl sulphate-polyacrylamide gel, and $\beta$-gal (arrow) was detected by western blotting (**d**). AAV, adeno-associated virus; $\beta$-gal, $\beta$-galactosidase; GAPDH, glyceraldehyde-3-phosphate dehydrogenase; H&E, hematoxylin and eosin; rAAV, recombinant adeno-associated virus; TA, tibialis anterior.

**Table 1** Gene transfer of rAAV2-CMVLacZ into canine skeletal muscles

| *Animal*[a] | | | *Injection*[b] | *β-Gal expression*[c] | | | *Cellular infiltration*[d] | | |
|---|---|---|---|---|---|---|---|---|---|
| | | | | *2 weeks* | *4 weeks* | *8 weeks* | *2 weeks* | *4 weeks* | *8 weeks* |
| *Injection at 2 days* | | | | 10 days | 30 days | 65 days | 10 days | 30 days | 65 days |
| 9223 | GR | F | ($8.2 \times 10^{11}$ vg/100 μl) | ± | − | − | ± | ± | ± |
| 3290 | B | M | ($1.5 \times 10^{12}$ vg/100 μl) | − | ± | − | + | ++ | + |
| 7690 | B | M | ($1.5 \times 10^{12}$ vg/100 μl) | ± | ± | − | + | ++ | ± |
| 0665 | B | M | ($2.2 \times 10^{13}$ vg/100 μl) | ± | − | − | + | ++ | ± |
| *Injection at 4 weeks* | | | | 13d | | | 13d | | |
| 7329 | B | F | ($1.0 \times 10^{12}$ vg/100 μl) | −, −, −, − | | | +, +, +, + | | |
| 4657 | B | F | ($1.0 \times 10^{12}$ vg/100 μl) | ±, − | | | +, ± | | |
| *Injection at 8 weeks* | | | | 10 days | 30 days | 59 days | 10 days | 30 days | 59 days |
| 02490 | B | M | ($5.0 \times 10^{12}$ vg/500 μl) | | −, −, − | | | ++, ++, + | |
| 0338 | GR | M | ($8.0 \times 10^{12}$ vg/500 μl) | ++ | − | − | + | ++ | + |
| FD89 | GR | F | ($8.0 \times 10^{12}$ vg/500 μl) | ± | − | − | ++ | + | + |
| *Injection at 10 weeks* | | | | 14 days | 28 days | | 14 days | 28 days | |
| 901[e] | B | M | ($5.0 \times 10^{10}$ vg/500 μl) | ± | ± | | − | + | |
| | | | ($5.0 \times 10^{11}$ vg/500 μl) | − | ± | | − | ++ | |
| *Injection at 12 weeks* | | | | 10 days | 30 days | 59 days | 10 days | 30 days | 59 days |
| FF04 | GR | M | ($8.0 \times 10^{12}$ vg/500 μl) | ± | − | − | ++ | + | ± |
| E566 | GR | M | ($8.0 \times 10^{12}$ vg/500 μl) | − | − | − | ++ | + | − |
| *Injection at 16 weeks* | | | | | 27 days | | | 27 days | |
| 02232 | B | M | ($5.0 \times 10^{13}$ vg/500 μl) | | −, −, − | | | ++, +, + | |
| *Injection at 6 months* | | | | 14 days | | | 14 days | | |
| 0065 | B | F | ($7.5 \times 10^{12}$ vg/500 μl) | ± | | | + | | |
| *Injection at 14 months* | | | | | 28 days | | | 28 days | |
| D01 | B | M | ($5.0 \times 10^{11}$ vg/500 μl) | | −, −, − | | | +, ±, + | |
| D03 | B | M | ($5.0 \times 10^{12}$ vg/500 μl) | | −, −, − | | | +, ++, ++ | |

[a]Canine species and sex: B, beagle; GR, golden retriever; M, male; F, female.
[b]Dosage per muscle: rAAV titer (vg) and injection volume (μl).
[c]β-Gal-positive fibers: −, 0; ±, <100; +, <300; ++, <1000; +++, >1000.
[d]Infiltrating cells: −, not detected; ±, few; +, moderate; ++, extensive.
[e]Two kinds of dosages of rAAV were injected into a dog.
In [c] and [d], individual results of the injected muscles were shown.

expression of the transferred gene (Table 1, dogs 3290, 7690 and 901). To determine whether contamination of cellular proteins in the stocks of AAV vectors lowers transduction efficiency, we tried three different AAV preparation protocols: (i) two-cycle CsCl density gradient ultracentrifugation, (ii) heparin column chromatography, or (iii) combination of them, and found that preparation using heparin column chromatography showed high levels of contamination of transgene products and cellular proteins (Supplementary Figure 1). CsCl ultracentrifugation efficiently eliminated contaminated empty viral particles. Combination of these two methods almost completely eliminated contaminated proteins. Nevertheless, all rAAV stocks showed high levels of β-gal expression in murine muscles (data not shown), but evoked cellular infiltration in normal canine muscles (Supplementary Figure 1).

To quantify the levels of infection and transduction of rAAV2-CMVLacZ in canine muscles, we isolated DNA and RNA from the injected muscles, and semiquantitatively evaluated rAAV genome copy numbers and the level of β-gal mRNA by PCR and reverse transcription (RT)-PCR, respectively. AAV vector genomes and β-gal mRNA were detected at 2, 4 and 8 weeks after the injection (Figures 2b and c). β-Gal protein, however, could not be detected by western blot at all stages after the injection (Figure 2d). These results suggest that canine myofibers were transduced by a rAAV2 *in vivo*, but the transduced cells were eliminated by the host's defense mechanisms.

### *rAAV-mediated gene transfer into canine muscles evoke both cellular and humoral immune response*

We next analyzed cell markers on infiltrating cells in the rAAV2-CMVLacZ-injected muscles (Figure 3a) at 2 weeks after the injection at 12 weeks. Numerous CD4+ or CD8+ T lymphocytes were detected in the interstitial spaces of the injected muscle. CD11b+ cells and B cells were also detected in the cluster of infiltrating cells. Furthermore, the expression of the major histocompatibility complex (MHC) class I and -II molecules were highly upregulated on both mononuclear cells and muscle fibers. IgG deposits were found in both the

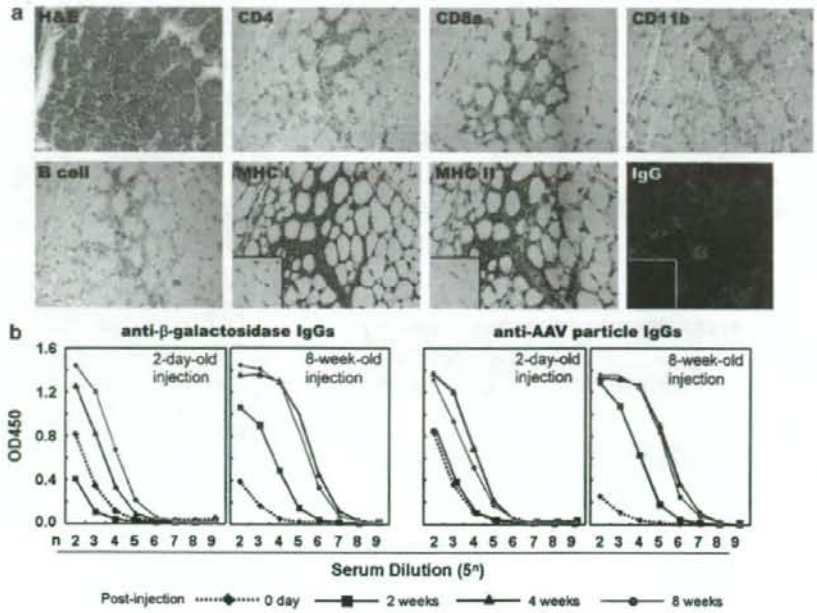


Figure 3 Immune responses were remarkably activated after rAAV2-mediated gene transfer into canine muscles. (a) Infiltrating cells in the rAAV2-CMVLacZ-injected canine TA muscles at 2 weeks after the injection. Serial cross-sections were immunostained with antibodies against canine CD4, CD8a, CD11b, B cell, MHC class I and -II, and IgGs. Insets show the noninjected muscles. Dog: FF04. Magnification: × 400. (b) Humoral immune responses against the transgene product and rAAV particle in the rAAV-treated dogs. Sera from dogs injected with rAAV2-CMVLacZ at 2 days and 8 weeks were analyzed for the presence of IgG antibodies against β-gal or AAV particle at 0, 2, 4 and 8 weeks after the injection, using ELISA. Dogs: 9223 and 0338. AAV, adeno-associated virus; β-gal, β-galactosidase; ELISA, enzyme-linked immunosorbent assay; MHC, major histocompatibility complex; rAAV, recombinant adeno-associated virus; TA, tibialis anterior.

cytoplasm of myofibers and the extracellular space in the rAAV-injected muscle. We next examined the antibodies against the transgene product or rAAV particles in the sera of rAAV-injected dogs (Figure 3b). The levels of serum IgGs that react β-gal protein or rAAV2 particle were gradually increased with time in both 2-day-old and 8-week-old injections. When injected at 8 weeks, the levels of IgGs against β-gal or rAAV2 increased from 2 weeks after the injection, and reached the peak at 4 weeks. When injected at 2 days, anti-β-gal or anti-AAV antibodies were not detected at 2 weeks after the injection, but had begun to increase at 4 weeks. The results would explain why the lacZ was expressed for a longer time, when injected at neonatal age (Table 1). These results suggest that cellular and humoral immune responses are elicited after the transfer of a rAAV2 into canine muscles.

### *Administration of a rAAV expressing no transgene into canine muscles*

Transduction of skeletal muscle by rAAV2-CMVLacZ presents two main foreign antigens, namely β-gal protein and AAV capsid to the host's immune system. To test which antigen is responsible for rapid elimination of transduced myofibers after rAAV-mediated gene transfer into canine muscle, we constructed a rAAV2 expressing no transgene, named rAAV2-LacZ-P(−), by removing the MCK promoter from the parental rAAV2-MCKLacZ (Figure 4a). We confirmed that the promoter-deleted rAAV2 expressed no β-gal in muscle after injection into skeletal muscles of normal mice ($5 \times 10^{11}$ vg/50 μl/site) (data not shown). Then, we injected the same titers of rAAV2-LacZ-P(−) and rAAV2-CMVLacZ, into skeletal muscles of normal adult beagles, and evaluated transduction efficiency by quantitative PCR of AAV genomes or histopathologically at 2 and 4 weeks post-injection. In 5 × 5 × 10 mm tissues of rAAV2-LacZ-P(−)-injected muscles, 1–10 pg of rAAV genomes were detected by PCR, whereas 500 fg to 5 pg of rAAV sequences were amplified in the injected muscles of rAAV2-CMVLacZ (Figures 2b and 4b). These results indicate that the promoter-deleted rAAV2 could successfully infect canine muscles and the viral genomes were retained stably in the fibers.

H&E staining showed that deletion of the MCK promoter greatly reduced the cellular infiltration into the rAAV2-LacZ-P(−)-injected muscles at 2 and 4 weeks after the injection, in contrast to the rAAV2-CMVLacZ-injected muscles (Figure 4). Even in a muscle sample in which vector genome was detected at the highest level by PCR, infiltrating cells were rarely found (sample 1c in Figures 4b and c). In addition, CD4+ or CD8+ cells were not detected in the rAAV2-LacZ-P(−)-injected muscles (data not shown). These results suggest that the transgene product but not AAV particle strongly elicits immune responses that subsequently eliminated transduced myofibers.

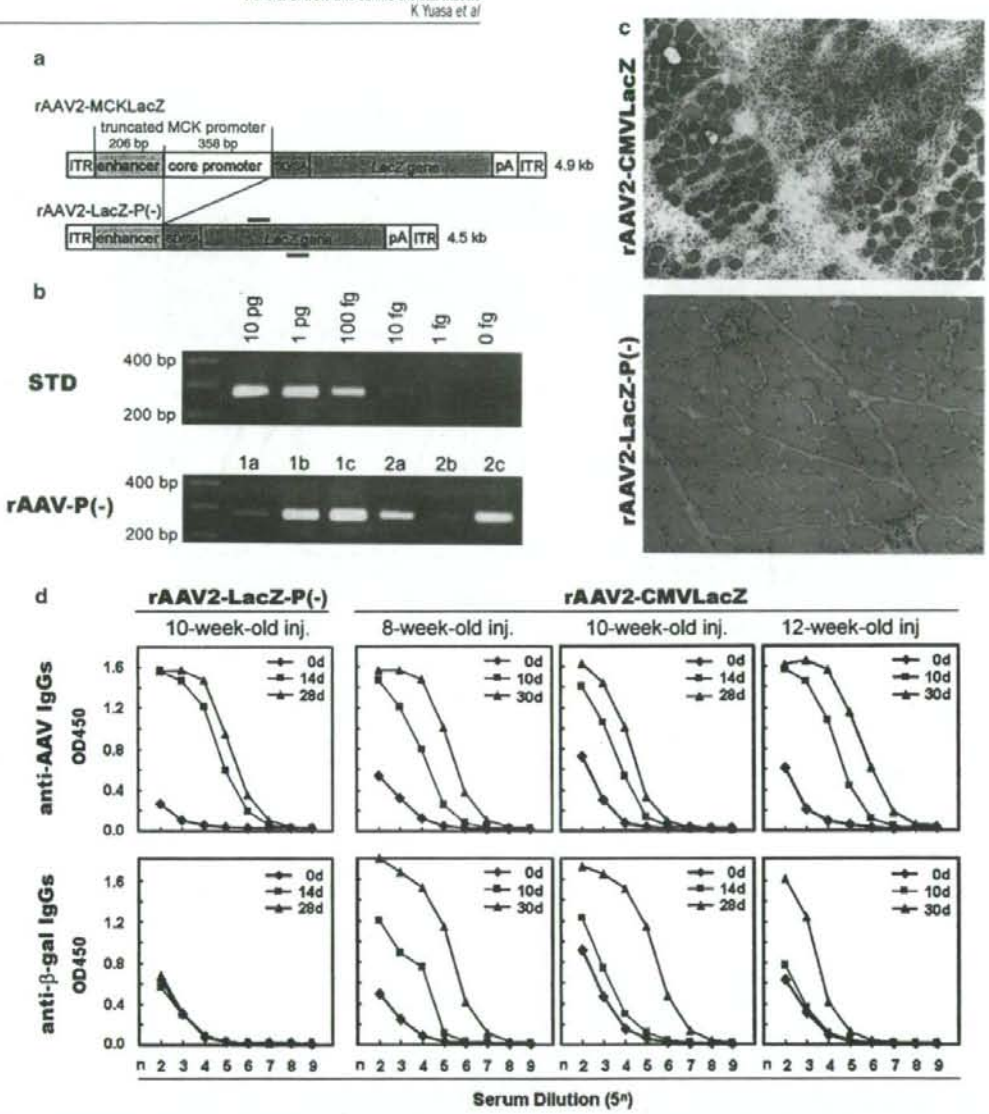


**Figure 4** Injection of the promoter-deleted rAAV2 showed negligible cellular infiltration in canine muscle. The promoter-deleted rAAV2, rAAV2-LacZ-P(−) ($5 \times 10^{12}$ vg/500 μl/site) was injected into skeletal muscles of 10-week-old beagle (dog 902), and the injected muscles and sera were analyzed at 2 and 4 weeks post-injection. (**a**) Schematic illustration of rAAV2-LacZ-P(−). Upper and lower bars correspond to primer positions used for detection of genome in Figure 4b. (**b**) Detection of rAAV genome DNA in the rAAV-LacZ-P(−)-injected canine muscles. Total DNA was extracted from the muscle sections, and *LacZ* DNA fragment (275 bp) was amplified from 200 ng of template DNA by PCR. Results at 2 weeks after the injection were shown. The numbers 1a–2c show individual identities of the muscle specimen divided into pieces. Vector genomes were detected in all samples, but amplified levels were different between muscle blocks. STD: quantity standard of AAV vector plasmid; rAAV-P(−): rAAV2-LacZ-P(−) genome. (**c**) Cellular infiltrations were rarely observed in the rAAV2-LacZ-P(−)-injected canine TA muscle (sample 1c). Canine muscles were injected with the rAAVs expressing β-gal or no transgene, and the muscle blocks were sectioned and stained with H&E staining at 2 weeks after the injection. All muscle samples from rAAV2-CMVLacZ (1a–2c) showed minimal cellular infiltration. Magnification: ×200. (**d**) Detection of antibodies against AAV particles and β-gal in the rAAV-treated dogs. Sera from dogs injected with rAAV2-LacZ-P(−) (dog 902) or rAAV2-CMVLacZ (dogs 0338, 901 and FF04, also see Table 1) were analyzed by using the ELISA technique for the presence of IgG antibodies against AAV particles and β-gal protein at 0, 2 and 4 weeks after the injection. AAV, adeno-associated virus; β-gal, β-galactosidase; ELISA, enzyme-linked immunosorbent assay; rAAV, recombinant AAV.

Next, we measured the anti-AAV IgG type antibodies in the serum of the treated dogs (Figure 4d). In the rAAV2-LacZ-P(−)-injected dog at 2 and 4 weeks after the injection, anti-AAV2 antibodies were detected at high levels similar to those in rAAV2-CMVLacZ-injected dogs, but antibodies against β-gal were undetectable. This indicates that antibodies against AAV particles were developed in rAAV2-LacZ-P(−)-injected dogs but did not lead to elimination of transduced cells.

### *Immunosuppression of the rAAV-injected dogs slightly improved the expression of the transgene*

To test whether immunosuppression could improve transduction by rAAV-2 in canine muscle, we daily administered cyclosporine to the rAAV2-CMVLacZ-injected dogs from −5 day of the injection until the sampling day of muscle specimens (Table 2A). Unexpectedly, β-gal expression in the injected muscles of cyclosporine-treated dogs was as low as that in the untreated dogs. Only the extensor digitorum longus (EDL) muscle of dog 403 expressed β-gal at a high level at 2 weeks after the injection, although a large number of infiltrating cells with CD4+ or CD8+ cells and upregulation of MHC class I and -II were detected (data not shown). In contrast, in the rAAV2-CMVLacZ-injected extensor carpi ulnaris (ECU) muscle of dog 403 at 2 weeks post-injection, β-gal expression was much lower than that in the EDL muscle. Thus, as a whole, cyclosporine alone could not effectively improve transduction of rAAV2-CMVLacZ.

Mycophenolate mofetil (MMF) suppresses the functions of T lymphocytes in a different way with cyclosporine. Therefore, to suppress immune responses more effectively, we treated the rAAV2-CMVLacZ-injected dogs both with MMF and cyclosporine. MMF was daily administrated from 0 day to the day of sampling (Figure 5 and Table 2B). This combined immunosuppression significantly increased the numbers of β-gal-expressing fibers, compared with those in the untreated muscles when examined at 2 weeks after the injection, but cellular infiltration was still observed. Some CD4+ or CD8+ cells and upregulation of MHC class I and -II in infiltrating cells and myofibers were detected in rAAV2-CMVLacZ-injected muscle (data not shown). After 4 weeks, β-gal expression significantly decreased together with increasing infiltrating cells. These results indicated that combination of cyclosporine and MMF could partially improve the transduction efficiency of a rAAV2 in canine muscles.

### *Immunological background of enhanced immune responses in dogs*

We next investigated possible differences in immune responses between mice and dogs, which might explain why rAAV2 injection evoked strong immune responses in canine muscles. To this end, we prepared single-cell suspension from spleens of untreated dogs or mice, stimulated them with AAV capsids and purified β-gal protein *in vitro*, and assayed the secretion of interferon-γ (IFN-γ) by enzyme-linked immunosorbent assay (ELISA; Table 3). We also stimulated the splenocytes with two major mitogens for T lymphocytes, concanavalin A (ConA) and phytohemagglutinin (PHA). When stimulated with ConA or PHA, canine splenocytes secreted much larger amount of IFN-γ into the culture medium than murine cells. Furthermore, canine cells secreted slightly higher levels of IFN-γ in response to β-gal or rAAV2 capsid proteins than murine cells. These results suggest that canine splenocytes are innately more susceptive to

**Table 2** Gene transfer of rAAV2-CMV-LacZ into canine skeletal muscles under immunosuppression

| *Animal*[a] | | | *Injection*[b] | *Cyclosporine* | *Expression*[c] | | *Infiltration*[d] | |
|---|---|---|---|---|---|---|---|---|
| *(A) Cyclosporine alone* | | | | | | | | |
| *Injection at 5 weeks* | | | | Dose/kg/day | 2 weeks | 4 weeks | 2 weeks | 4 weeks |
| *601* | B | M | ($6.0 \times 10^{12}$ vg/500 μl) | 20 mg | − | | + | |
| *Injection at 8 weeks* | | | | | | | | |
| 1103 | B | M | ($5.0 \times 10^{10}$ vg/500 μl) | 25 mg | −, − | ±, − | ±, ± | +, − |
| 1102 | B | M | ($6.0 \times 10^{11}$ vg/500 μl) | 25 mg | ±, − | ±, − | +, ± | +, + |
| *Injection at 11 weeks* | | | | | | | | |
| 403 | B | M | ($7.7 \times 10^{12}$ vg/500 μl) | 20 mg | +++, +[e] | +, ± | +, + | +, + |
| 703 | B | M | ($5.0 \times 10^{12}$ vg/500 μl) | 50 mg | − | | ± | |
| *Animal*[a] | | | *Injection*[b] | *Cyclosporine, MMF* | *Expression*[c] | | *Infiltration*[d] | |
| *(B) Cyclosporine and MMF* | | | | | | | | |
| *Injection at 10 weeks* | | | | Dose/kg/day | 2 weeks | 4 weeks | 2 weeks | 4 weeks |
| VC1XE | B | M | ($5.0 \times 10^{11}$ vg/500 μl) | 25 mg, 30 mg | ++, + | ±, + | +, ± | +, ++ |
| TC2XE | B | M | ($5.0 \times 10^{12}$ vg/500 μl) | 25 mg, 30 mg | ±, + | +, − | +, + | ++, + |
| *Injection at 12 weeks* | | | | | | | | |
| 1902 | B | M | ($5.0 \times 10^{11}$ vg/500 μl) | 25 mg, 30 mg | + | ++ | ± | ± |

Abbreviations: B, beagle; ECU, extensor carpi ulnaris; EDL, extensor digitorum longus; F, female; M, male; MMF, mycophenolate mofetil.
[a–d]See Table 1.
[e]+++ was seen in an EDL muscle, whereas + was in an ECU muscle.
In [c] and [d], individual results of the injected muscles were shown.

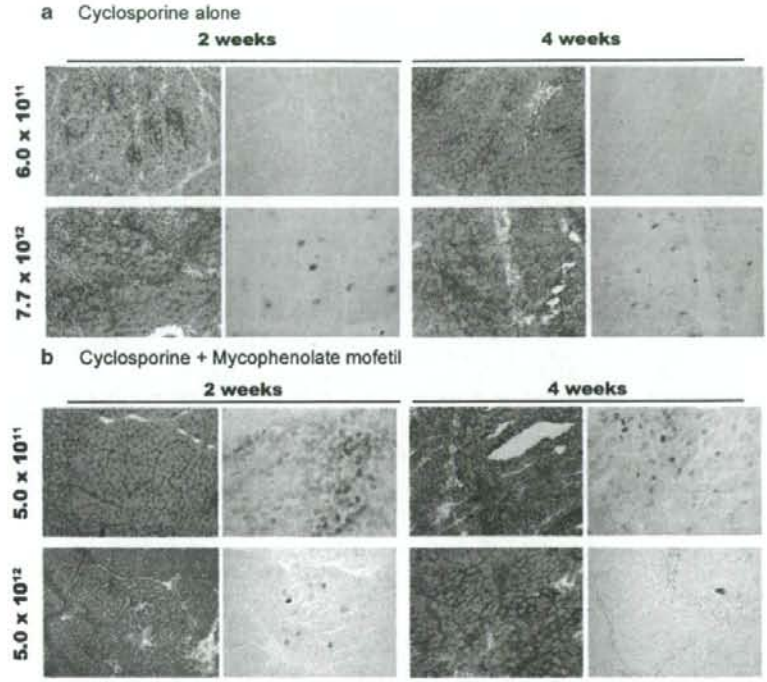


**Figure 5** Combined immunosuppression partially improved transgene expression in rAAV2-mediated gene transfer into canine muscle. Representative H&E and X-gal stainings showing improvement in the transduction efficiencies of rAAV2-CMVLacZ at 2 and 4 weeks after the injection under immunosuppression (also see Table 2). The rAAV ($5.0 \times 10^{11}$–$7.7 \times 10^{12}$ vg/site) was injected into TA and ECU muscles of beagles, and the dogs were daily treated with cyclosporine alone (**a**) or combination of cyclosporine and MMF (**b**). The muscle of dog 1102 was injected with rAAV at a dose of $6.0 \times 10^{11}$ vg (upper panels in **a**). Dog 403 was injected with rAAV at a titer of $7.7 \times 10^{12}$ vg; beagle VC1XE was injected with rAAV at a dose of $5.0 \times 10^{11}$ vg (upper panels in **b**). TC2XE was injected with $5.0 \times 10^{12}$ vg rAAV (lower panels in **b**). Magnification: × 100. ECU, extensor carpi ulnaris; H&E, hematoxylin and eosin; MMF, mycophenolate mofetil; rAAV, recombinant adeno-associated virus; TA, tibialis anterior; X-gal, 5-bromo-4-chloro-3-indolyl-β-D-galactopyranoside.

immunogens or mitogens than murine ones, and this immunological difference might underlie severer immune responses to rAAV2 injection in dogs than in mice.

## Discussion

rAAV2 drives a long-term expression of microdystrophin genes in skeletal muscles of dystrophic mice,[9] therefore it is an attractive tool for treatment of DMD. To test the efficacy and safety of rAAV-mediated gene transfer into skeletal muscle of larger animal models, we directly injected rAAV2 encoding β-gal into skeletal muscle of normal dogs and examined the β-gal expression at several time points. Unexpectedly, we found that rAAV2-mediated gene transfer elicits strong immune responses against the transgene product in canine skeletal muscles. The mechanisms of enhanced immune reactions after rAAV2 injection seen in normal dogs need to be clarified before applying rAAV-mediated gene therapy to boys with DMD.

### *rAAV2 efficiently transduces canine muscle* in vitro *but not* in vivo

In mice, β-gal expression is maintained for a long time after rAAV-CMVLacZ injection into muscle.[8] In contrast, low levels of β-gal expression and numerous infiltrating cells were observed in the rAAV2-CMVLacZ-injected canine muscle. Surprisingly, rAAV2 infected and transduced canine myotubes more effectively than murine myotubes *in vitro* (Figure 1). Therefore, we conclude that the low expression of the transgene in dog muscle is not due to the lack of receptors for the AAV2 on canine muscle fibers.

### *Cytotoxic immune response against the transgene product*

Immunosuppression reduced cellular infiltration in rAAV2-CMVLacZ-injected muscle and partially rescued the β-gal expression in myofibers, suggesting that cytotoxic T-cell responses to transduced muscle fibers are largely responsible for the elimination of β-gal-positive myofibers in the injected muscle. Furthermore, intramuscular injection of the promoter-deleted rAAV2, which can infect the muscle (Figure 4) but express no β-gal (data not shown), induced much less cellular infiltration in canine muscle than the rAAV2-CMVLacZ. This observation suggests that massive destruction of the transduced muscle cells is mainly due to cellular immunity against the transgene product but not against AAV capsid proteins.

Table 3 IFN-γ release assay in murine and canine splenocytes

| *Immunogen* | | *IFN-γ (pg/ml)* | |
|---|---|---|---|
| | | *Mouse* | *Dog* |
| None | — | <9.4 | <32 |
| β-gal | 500 ng | <9.4 | <32 |
| | 5 μg | <9.4 | 166±5 |
| | 50 μg | 334±20 | 1316±122* |
| rAAV | $1\times10^{8}$ vg | <9.4 | <32 |
| | $1\times10^{9}$ vg | <9.4 | <32 |
| | $1\times10^{10}$ vg | <9.4 | 59±19 |
| ConA | 5 ng | <9.4 | <32 |
| | 50 ng | <9.4 | 4928±162 |
| | 500 ng | 6750±132 | 57 567±6374* |
| | 5 μg | 4095±474 | 65 050±5467* |
| PHA | 50 ng | <9.4 | 49±7 |
| | 500 ng | <9.4 | 5227±479 |
| | 5 μg | 2683±253 | 43 833±4488* |
| | 50 μg | 5453±349 | 60 133±6616* |

Abbreviations: β-gal, β-galactosidase; ConA, concanavalin A; ELISA, enzyme-linked immunosorbent assay; IFN-γ, interferon-γ; PHA, phytohemagglutinin; rAAV, recombinant adeno-associated virus.
Splenocytes were stimulated with various doses of immunogens, such as β-gal, rAAV particle (rAAV), ConA and PHA, and secreted level of murine and canine IFN-γ in culture medium were measured by ELISA. Data are expressed as means±s.d., and significant differences (*$P<0.01$) between mouse and dog were shown.

There have been several papers reporting studies of rAAV-based gene transfer into canine skeletal muscle. Most of them were gene transfer studies for hemophilia B dogs, and reported that cellular immune responses against Factor IX, were nearly absent in dog models of hemophilia B.[15–19] The difference between studies of hemophilia and ours might be explained by the antigenicity of the transgene products. When we injected rAAV2-CMVM3 expressing M3 microdystrophin[7] into skeletal muscles of normal dogs, cellular infiltration was considerably reduced (data not shown), indicating that lowering the immunogenicity of therapeutic genes is important to improve the efficiency of gene therapy. In addition, nonsecreted, intracellular proteins might tend to evoke cellular immunity, compared with secreted proteins, like Factor IX.

We showed quite low expression of β-gal in rAAV2-CMVLacZ-injected muscle, whereas AAV genome and *LacZ* mRNA in rAAV-CMVLacZ-injected muscle were detected even at 8 weeks after the injection (Figure 2). The gap between *LacZ* mRNA level and β-gal protein cannot be fully explained at present. This might be simply due to time lag between transcription and translation of the transgene, or translation of β-gal might be repressed in inflammatory muscles.

### *Immunity against AAV2 capsid in dogs and humans*

Promoter-deleted rAAV2 injection did develop antibodies against the AAV2 capsid after the injection into the skeletal muscle (Figure 4d), but did not evoke strong immune reactions in muscle, suggesting that cytotoxic T cells targeting the AAV2 capsid protein were not or minimally activated. This observation is consistent with the previous reports that cellular immune response to the AAV capsid was absent in hemophilia B dogs.[17–19] However, it is still unclear whether cellular immune response against the AAV2 capsid proteins is completely absent in dogs. Because even a low-level response could be problematic in the clinic, immunity to the AAV2 capsid proteins should be carefully monitored in dog models. In contrast, it has been recently reported that liver-directed rAAV2 transfer for human trial of hemophilia B led to destruction of transduced hepatocytes by cell-mediated immunity targeting the AAV2 capsid.[13] The authors suggest that T-cell immunity against the AAV2 particles might be associated with peptide sequence within the AAV2 capsid which had a high predicted binding potential to *B*0702* molecule of human MHC class I. This may explain why cell-mediated immune response against the AAV2 capsid protein was activated in humans.

### *Backgrounds of immune responses in dogs and mice*

We measured the levels of IFN-γ secreted from canine or murine splenocytes after stimulation with β-gal, rAAV2 viral particles, ConA or PHA *in vitro*. Although biological activities (e.g., $EC_{50}$) of canine IFN-γ might be different from those of murine IFN-γ, it is likely that canine immune system is more sensitive to foreign antigens, such as β-gal. We also showed that canine splenocytes secrete much larger quantity of INF-γ than murine splenocytes when exposed to ConA or PHA. The higher levels of overall immune activation in dogs than in mice might be responsible for rapid development of immune response to rAAV2-mediated gene transfer into canine skeletal muscle, and might be partly explained by the different sanitary status of murine and canine colonies.

Antigen-presenting cells (APCs) in skeletal muscle play an important role in development of immunity to transgene products.[8,20] Therefore, it is also possible that rAAV transduces APCs more efficiently in dogs than in mice.

### *Threshold hypothesis for detrimental immune reaction*

A previous study showed that systemic delivery of rAAVs, such as isolated limb perfusion (ILP) elicited less immune response than local injection.[19] Other study in hemophilia B dogs suggested that local Factor IX antigen dose in rAAV-injected muscles would be a critical parameter for risk of developing neutralizing antibody in dog.[18] The authors discussed that vector dose of $2\times10^{12}$ vg/site and $8.5\times10^{12}$ vg/kg might represent a threshold at which an inhibitory anti-Factor IX was or was not induced. These observations might indicate that the local concentration of the rAAV particles and its gene product is an important factor for establishment of immunity against rAAVs. Direct injection of rAAV2-CMVLacZ particles into muscle might cause the excessive expression of β-gal within a small area, and thereby mount strong cellular immune responses against gene products. Recently, we observed that pseudo-typed rAAV2/8 efficiently delivered the transgene into canine muscle (Ohshima *et al.*, unpublished observation). The expression of β-gal from rAAV8-CMVLacZ distributed more widely, and more evenly within the muscle than rAAV2-CMVLacZ after direct injection into canine

muscle. We hypothesize that widespread transduction of myofibers at a low dose of a rAAV2/8 could escape the establishment of immunity against the transgene products. New serotypes of AAVs, such as AAV8 or AAV9 can deliver the transgene into musculature of the whole body via circulation.[21,22] These vectors might overcome the immunological problems that we encountered in rAAV2-mdiated gene transfer into canine muscles.

In conclusion, we found that intramuscular administration of rAAV2-CMVLacZ elicited rapid and severe immune responses against the transgene product in wild-type dogs. This has not been observed in mice. It is important to understand well the mechanisms of immune reactions observed in dogs to circumvent immunological limitations, which might stand in our way in preclinical and clinical trials for DMD.

## Materials and methods

### *Construction and production of rAAVs*

We used rAAV2-CMVLacZ and rAAV2-CMVM3, which harbors the *LacZ* gene or microdystrophin M3 driven by the CMV promoter, respectively.[3,7,8] To improve the expression efficiency of the LacZ gene in rAAV2-CMVLacZ, a chimeric intron (human $\beta$-globin splicing donor and immunoglobulin splicing acceptor, Promega, Madison, WI, USA) is inserted between CMV promoter and the LacZ gene.[8] rAAV2-LacZ-P(−) was generated by deleting the truncated MCK promoter (358 bp) from rAAV2-MCKLacZ, leaving the MCK enhancer intact.[8] We confirmed that rAAV2-LacZ-P(−) could not express $\beta$-gal in murine muscle cells both *in vitro* and *in vivo* (data not shown). The rAAV was produced by a plasmid triple-cotransfection method,[23] purified by two CsCl density gradient centrifugations[24] and/or heparin column chromatography,[25] and titrated by a quantitative DNA dot-blot assay.

### *Administration of rAAVs into canine or murine skeletal muscles and isolation of the injected muscles*

Experimental dogs were wild-type littermates of beagle-based CXMD$_J$ breeding colony at National Center of Neurology and Psychiatry (NCNP; Tokyo, Japan),[10,11] or golden retriever muscular dystrophy colony at Murdoch University (Perth, Australia).[26] All animals were cared and treated in accordance with the guidelines approved by Ethics Committee for Treatment of Laboratory Animals at NCNP or Animal Ethics Committee at Murdoch University, where three fundamental principles (replacement, reduction and refinement) were also considered. When a rAAV was injected into dogs, the animals were not vaccinated to relive influences of immune response by vaccination. rAAVs were injected intramuscularly at ages from 2 days to 14 months, and the muscles were isolated after 2, 4 and 8 weeks. Surgeries were done under anesthesia with isoflurane, as described previously.[27] Briefly, the ECU, tibialis anterior (TA) or EDL muscles were surgically exposed and two marker sutures were placed on the mid-belly of the muscle at proximal and distal positions apart approximately 20 mm. rAAV ($5 \times 10^{10}$–$8 \times 10^{12}$ vg in 100 or 500 $\mu$l) or phosphate-buffered saline (PBS) was injected slowly into the muscles between two markers along the length. In biopsy and necropsy, the entire muscle blocks with two sutures were removed, divided into some pieces, and immediately frozen in isopentane precooled with liquid nitrogen. rAAV ($5 \times 10^{11}$ vg/50 $\mu$l) was also injected into TA muscles of C57BL/10 mice at 5 weeks, and the muscles were isolated at 2 or 4 weeks after the injection.

### *Immunosuppression*

To suppress immune reaction, we treated rAAV-injected dogs with cyclosporine alone or cyclosporine combined with MMF for immunosuppression. Cyclosporine (NEORAL capsules; Novartis, Basel, Switzerland) was administrated orally at doses of 20–50 mg/kg/day and daily from −5 day of the injection. MMF (CellCept capsules, Roche Pharmaceuticals, Nutley, NJ, USA) was administrated orally at a dose of 30 mg/kg/day and daily from 0 day of the injection.

### *Histological and immunohistochemical analysis*

Transverse cryosections from the rAAV-injected muscles were stained with H&E or 5-bromo-4-chloro-3-indolyl-$\beta$-D-galactopyranoside (X-Gal).[8]

Immunohistochemistry was performed as described previously.[8] Cryosections were incubated with the following antibodies: mouse monoclonal antibodies against canine CD4 (CA13.1E4, Serotec, Oxford, UK), canine CD8a (CA9.JD3, Serotec), canine CD11b (CA16.3E10, Serotec), canine B cells (CA2.1D6, Serotec), class I major histocompatibility antigen (H58A, VMRD, Pullman, WA, USA) and canine MHC class II (CA2.1C12, Serotec), and fluorescein-conjugated goat affinity-purified antibody to dog IgG (whole molecule) (Cappel, Solon, OH, USA). The primary antibodies were detected using VECTASTAIN ABC kit (Vector Laboratories, Burlingame, CA, USA), then visualized with diaminobenzidine, and counterstained with methyl green.

### In vitro *infection assay in primary myotubes*

Canine or murine primary myoblasts were isolated and differentiated into myotubes, according to the previously published protocol[28] with some modifications. Briefly, muscle mass was removed from dogs or mice at 0 day to 2 weeks, weighted and minced. Cells were enzymatically dissociated in PBS (4 ml per g of tissue) containing dispase II (2.4 IU/ml, Godo Shusei, Tokyo, Japan) and Collagenase type XI (0.2%, Sigma, St Louis, USA), and 2.5 mM $CaCl_2$. The slurry was incubated at 37°C for 90–120 min with trituration every 15 min, and then passed through 100 $\mu$m pore mesh. The filtrate was spun at 350 *g*, and the pellet was resuspended in growth medium (F-10 medium with 20% fetal bovine serum (FBS) and 2.5 ng/ml human basic fibroblast growth factor (Sigma)). The cell suspension was then plated on non-coated dishes for 90 min, and non-adherent cells were collected and plated onto new dishes. After several repeats of this pre-plating procedure, myoblasts were enriched. To assess transduction efficiency of a rAAV in primary myotubes, the same numbers of myoblasts ($2 \times 10^4$ cells/well) were plated onto 24-well plates and maintained for a few days in differentiation medium (Dulbecco's modified Eagle's medium with 5% FBS and 10 $\mu$g/ml human insulin (Sigma)), and then cultured in the presence of rAAV2-CMVLacZ ($2 \times 10^8$–$2 \times 10^{11}$ vg/well), or co-infected with the rAAV2 and adenovirus Ad5-dlX[3]

($1 \times 10^7$ plaque-forming unit (PFU)/ml). After 2 days, cells were stained with X-Gal.

### *Quantification of rAAV genome in canine muscle*

To quantify rAAV genomes, muscle sections were digested with proteinase K, followed by phenol/chloroform extraction and isopropanol precipitation. The DNA pellet was resuspended in TE buffer, and amplified by PCR with following primer sets: 5′-ccacgctgttttgacctccatag-3′ (downstream of transcription start site in the CMV promoter) and 5′-gtacaattccgcagcttttagagc-3′ (upstream of the *LacZ* gene) for rAAV2-CMVLacZ (the PCR product is 244 bp, illustrated in Figure 1a); 5′-gcagttatctggaagat cagg-3′ and 5′-cataaccaccacgctcatcg-3′ (within the *LacZ* gene) for rAAV2-LacZ-P(−) (the PCR product is 275 bp, illustrated in Figure 4a). As an internal control, the canine calmodulin gene II (CaMII; GenBank accession no. D12622) was amplified with following primers: 5′-gagaggactcatccaaggtcacac-3′ and 5′-tcagaaaccacggcat cagg-3′. AAV vector plasmids for rAAV2-CMVLacZ or rAAV2-LacZ-P(−) were served as a quantity control for standard amplification.

### *RT-PCR for transgene mRNAs*

Total RNA was isolated from muscle sections using RNAqueous-Micro kit (Ambion, TX, USA). Then first-strand cDNA was synthesized using First-Strand cDNA Synthesis Kit (GE Healthcare UK Ltd, Buckinghamshire, UK). mRNA of rAAV2-CMVLacZ was detected using the same primers used for genomic DNA (Figure 1a). The amplified product is 178 bp. As an internal control glyceraldehyde-3-phosphate dehydrogenase mRNA (GenBank accession no. AB038240) was amplified using the following primer set: 5′-tcatctctgctccttctgctgat-3′ and 5′-ggctagaggagccaagcagtt-3′.

### *Western blot analysis*

Muscle extracts were prepared from rAAV-injected canine muscles, separated on 7.5% sodium dodecyl sulfate-polyacrylamide gels, and then transferred onto polyvinylidene fluoride membranes, as described previously.[8] β-Gal protein was detected by rabbit polyclonal anti-β-gal antibody (Cappel).

### *ELISA*

ELISA were performed as described previously.[8] The microtiter plate was precoated with β-gal, rAAV2-CMVLacZ or rAAV2-LacZ-P(−), incubated with the sera from dogs, and then reacted with a 1/5000 dilution of peroxidase-conjugated rabbit anti-dog IgG (whole molecule) (Sigma). Reactivity was determined by the color reaction of 3,3′,5,5′,-tetramethylbenzidine (TMBZ).

### *IFN-γ release assay*

Spleen cells were isolated from C57BL/6 mice or beagle dogs, which were untreated with rAAVs. Splenetic cells were dissociated physically and passed through 100 μm filters. After removal of red blood cells using 0.83% ammonium chloride buffer (Sigma), splenocytes were cultured in RPMI medium containing 10% FBS at a density of $2 \times 10^6$ cells/well in 24-well plates for 2 days in the presence of various antigens: β-gal (500 ng to 50 μg), rAAV2-CMVLacZ ($1 \times 10^8$–$1 \times 10^{10}$ vg), ConA (5 ng to 5 μg, GE Healthcare Bio-Science) and phytohemagglutinin (50 ng to 50 μg, Sigma). The supernatant of the culture was assayed for the secretion of IFN-γ using Mouse or Canine IFN-γ Quantikine ELISA Kit (R&D Systems, Minneapolis, MN, USA). The amounts of canine or murine IFN-γ were calibrated using recombinant canine or murine IFN-γ proteins as standards, respectively, according to manufacturer's instructions. Results are given as means with standard deviation (s.d.) of three experiments. Data were first evaluated by *F*-test. When equality of variances was shown, *t*-test was used to evaluate the statistical significance. When rejected, Aspin–Welch-test was used.

## Acknowledgements

We are grateful to Dr Katsujiro Sato, Dr Yasushi Mochizuki, Dr Naoko Yugeta, Dr Akiyo Nishiyama, Dr Madoka Ikemoto, Dr Michiko Wada, Ms Kazue Kinoshita, Ms Ryoko Nakagawa, Mr Satoru Masuda, Dr Masayuki Tomohiro and Dr Yoshiki Shimatsu for technical assistance. We also thank Mr Hideki Kita and Mr Shinichi Ichikawa and other staff of JAC Co. for care and management of experimental animals. This work is supported by Grants-in-Aid for Scientific Research for Research on Nervous and Mental Disorders (10B-1, 13B-1, 16B-3) and Health Sciences Research Grants for Research on Human Genome and Gene Therapy (H10-genome-015, H13-genome-001, H16-genome-003) from the Ministry of Heath, Labor and Welfare of Japan, and Grant-in-Aid for Scientific Research (B) from the Ministry of Education, Culture, Sports, Science and Technology (MEXT). A part of this work in Musashino University is supported by High-Tech Research Center Project for Private Universities: matching fund subsidy from MEXT, 2004.

## References

1 Emery AEH. *Duchenne Muscular Dystrophy*, 2nd edn. Oxford University Press: Oxford, 1993.
2 Fisher KJ, Jooss K, Alston J, Yang Y, Haecker SE, High K *et al.* Recombinant adeno-associated virus for muscle directed gene therapy. *Nat Med* 1997; **3**: 306–312.
3 Yuasa K, Miyagoe Y, Yamamoto K, Nabeshima Y, Dickson G, Takeda S. Effective restoration of dystrophin-associated proteins *in vivo* by adenovirus-mediated transfer of truncated dystrophin cDNAs. *FEBS Lett* 1998; **425**: 329–336.
4 Harper SQ, Hauser MA, Dellorusso C, Duan D, Crawford RW, Phelps SF *et al.* Modular flexibility of dystrophin: implications for gene therapy of Duchenne muscular dystrophy. *Nat Med* 2002; **8**: 253–261.
5 Watchko J, O'day T, Wang B, Zhou L, Tang Y, Li J *et al.* Adeno-associated virus vector-mediated minidystrophin gene therapy improves dystrophic muscle contractile function in *mdx* mice. *Hum Gene Ther* 2002; **13**: 1451–1460.
6 Fabb SA, Wells DJ, Serpente P, Dickson G. Adeno-associated virus vector gene transfer and sarcolemmal expression of a 144 kDa micro-dystrophin effectively restores the dystrophin-associated protein complex and inhibits myofibre degeneration in nude/*mdx* mice. *Hum Mol Genet* 2002; **11**: 733–741.
7 Sakamoto M, Yuasa K, Yoshimura M, Yokota T, Ikemoto T, Suzuki M *et al.* Micro-dystrophin cDNA ameliorates dystrophic phenotypes when introduced into *mdx* mice as a transgene. *Biochem Biophys Res Commun* 2002; **293**: 1265–1272.

8 Yuasa K, Sakamoto M, Miyagoe-Suzuki Y, Tanouchi A, Yamamoto H, Li J *et al*. Adeno-associated virus vector-mediated gene transfer into dystrophin-deficient skeletal muscles evokes enhanced immune response against the transgene product. *Gene Therapy* 2002; **9**: 1576–1588.

9 Yoshimura M, Sakamoto M, Ikemoto M, Mochizuki Y, Yuasa K, Miyagoe-Suzuki Y *et al*. AAV vector-mediated microdystrophin expression in a relatively small percentage of *mdx* myofibers improved the *mdx* phenotype. *Mol Ther* 2004; **10**: 821–828.

10 Shimatsu Y, Katagiri K, Furuta T, Nakura M, Tanioka Y, Yuasa K *et al*. Canine X-linked muscular dystrophy in Japan ($CXMD_J$). *Exp Animals* 2003; **52**: 93–97.

11 Shimatsu Y, Yoshimura M, Yuasa K, Urasawa N, Tomohiro M, Nakura M *et al*. Major clinical and histopathological characteristies of canine X-linked muscular dystrophy in Japan, $CXMD_J$. *Acta Myologica* 2005; **24**: 145–154.

12 Valentine BA, Cooper BJ, Cummings JF, De Lahunta A. Canine X-linked muscular dystrophy: morphologic lesions. *J Neurol Sci* 1990; **97**: 1–23.

13 Manno CS, Arruda VR, Pierce GF, Glader B, Ragni M, Rasko J *et al*. Successful transduction of liver in hemophilia by AAV-Factor IX and limitations imposed by the host immune response. *Nat Med* 2006; **12**: 342–347.

14 Fisher KJ, Gao GP, Weitzman MD, DeMatteo R, Burda JF, Wilson JM. Transduction with recombinant adeno-associated virus for gene therapy is limited by leading-strand synthesis. *J Virol* 1996; **70**: 520–532.

15 Herzog RW, Yang EY, Couto LB, Hagstrom JN, Elwell D, Fields PA *et al*. Long-term correction of canine hemophilia B by gene transfer of blood coagulation factor IX mediated by adeno-associated viral vector. *Nat Med* 1999; **5**: 56–63.

16 Fields PA, Kowalczyk DW, Arruda VR, Armstrong E, Mccleland ML, Hagstrom JN *et al*. Role of vector in activation of T cell subsets in immune responses against the secreted transgene product factor IX. *Mol Ther* 2000; **1**: 225–235.

17 Herzog RW, Mount JD, Arruda VR, High KA, Lothrop Jr CD. Muscle-directed gene transfer and transient immune suppression result in sustained partial correction of canine hemophilia B caused by a null mutation. *Mol Ther* 2001; **4**: 192–200.

18 Herzog RW, Fields PA, Arruda VR, Brubaker JO, Armstrong E, Mcclintock D *et al*. Influence of vector dose on factor IX-specific T and B cell responses in muscle-directed gene therapy. *Hum Gene Ther* 2002; **13**: 1281–1291.

19 Arruda VR, Stedman HH, Nichols TC, Haskins ME, Nicholson M, Herzog RW *et al*. Regional intravascular delivery of AAV-2-F.IX to skeletal muscle achieves long-term correction of hemophilia B in a large animal model. *Blood* 2005; **105**: 3458–3464.

20 Zhang Y, chirmule N, Gao G, Wilson J. CD40 ligand-dependent activation of cytotoxic T lymphocytes by adeno-associated virus vectors *in vivo*: role of immature dendritic cells. *J. Virol* 2000; **74**: 8003–8010.

21 Wang Z, Zhu T, Qiao C, Zhou L, Wang B, Zhang J *et al*. Adeno-associated virus serotype 8 efficiently delivers genes to muscle and heart. *Nat Biotechnol* 2005; **23**: 321–328.

22 Inagaki K, Fuess S, Storm TA, Gibson GA, Mctiernan CF, Kay MA *et al*. Robust systemic transduction with AAV9 vectors in mice: efficient global cardiac gene transfer superior to that of AAV8. *Mol Ther* 2006; **14**: 45–53.

23 Xiao X, Li J, Samulski RJ. Production of high-titer recombinant adeno-associated virus vectors in the absence of helper adenovirus. *J Virol* 1998; **72**: 2224–2232.

24 Snyder R, Xiao X, Samulski RJ. Production of recombinant adeno-associated viral vectors. In: Dracopoli N, Haines J, Korf B, Morton C, Seidman C, Seidman JG, Smith D (eds). *Current Protocols in Human Genetics*. John Wiley & Sons Ltd: New York, 1996, pp 12.1.1–12.2.23.

25 Auricchio A, Hildinger M, O'connor E, Gao GP, Wilson JM. Isolation of highly infectious and pure adeno-associated virus type 2 vectors with a single-step gravity-flow column. *Hum Gene Ther* 2001; **12**: 71–76.

26 Howell JM, Fletcher S, Kakulas BA, O'hara M, Lochmuller H, Karpati G. Use of the dog model for Duchenne muscular dystrophy in gene therapy trials. *Neuromuscul Disord* 1997; **7**: 325–328.

27 Howell JM, Lochmuller H, O'hara A, Fletcher S, Kakulas BA, Massie B *et al*. High-level dystrophin expression after adeno-virus-mediated dystrophin minigene transfer to skeletal muscle of dystrophic dogs: prolongation of expression with immuno-suppression. *Hum Gene Ther* 1998; **9**: 629–634.

28 Rando TA, Blau HM. Primary mouse myoblast purification, characterization, and transplantation for cell-mediated gene therapy. *J Cell Biol* 1994; **125**: 1275–1287.

Supplementary Information accompanies the paper on Gene Therapy website (http://www.nature.com/gt)